Distinct responses of two hepatocellular carcinoma cell lines of a similar origin to immunotherapies targeting regulatory or effector T cells

YUJI NAGAYAMA[1], WATARU HASE[1], YASUHIDE MOTOYOSHI[1,2], OHKI SAITOH[1], RINTAROH SOGAWA[1] and KAZUHIKO NAKAO[2]

[1]Department of Medical Gene Technology, Atomic Bomb Disease Institute, [2]Department of Medical and Dental Sciences, Graduate School of Biomedical Sciences, Nagasaki University, 1-12-4 Sakamoto, Nagasaki 852-8523, Japan

Received January 23, 2007; Accepted February 26, 2007

Abstract. Balance between effector T cells (Teff) and regulatory T cells (Treg) appears to be very crucial for effective anti-tumor immunotherapy. The therapeutic efficacies of enhancement of Teff and suppression of Treg were compared between two murine hepatoma cell lines of a similar origin, MH129 and MH134. Enhancement of Teff was achieved by infection of tumor cells with adenovirus expressing glucocorticoid-induced tumor necrosis factor receptor-related protein (GITR), and suppression of Treg, by depletion of $CD4^+CD25^+$ naturally occurring Treg by administration of anti-CD25 monoclonal antibody (PC61) or low-dose cyclophosphamide. Our data show that MH129 cells were susceptible to Treg depletion but resistant to GITR expression, and *vice versa* for MH134 cells. Thus, in MH129 cells, injection of PC61 prior to or after tumor cell inoculation completely or partially, respectively, eradicated tumor growth. Low-dose cyclophosphamide administered after tumor cell inoculation also delayed tumor growth. However, GITR expression either *in vitro* or *in vivo* exhibited little effect. In contrast, in MH134 cells, PC61 induced partial tumor growth delay only when injected prior to tumor cell inoculation, and low-dose cyclophosphamide showed no effect, but GITR, particularly when administered *in vitro*, inhibited tumor growth. An additive effect of PC61 and GITR was observed only in MH134 cells. The ratios of peripheral $CD4^+CD25^+$ to $CD4^+$ T cells remained unaltered during the experimental course in both tumor models. From these results we speculate that this different sensitivity may be due to a difference in relative induction levels of Teff versus Treg, not due to different immunogenicity or different kinetics of peripheral Treg, between the two tumor models. Future studies identifying antigen(s) or epitope(s) specific for Teff and Treg in these tumor cell lines are necessary as analysis of the immune response to such antigen(s) or epitope(s) may in general help predict the relative efficacy of different immunotherapies against distinct tumors.

Correspondence to: Dr Yuji Nagayama, Department of Medical Gene Technology, Atomic Bomb Disease Institute, Nagasaki University Graduate School of Biomedical Sciences, 1-12-4 Sakamoto, Nagasaki 852-8523, Japan
E-mail: nagayama@nagasaki-u.ac.jp

Key words: effector T cells, $CD4^+CD25^+$ regulatory T cells, GITRL, cyclophosphamide, PC61

Introduction

It is well known that most tumor cells possess tumor-associated antigens, many of which are found as non-mutated self-components (1). These tumor antigens however generally fail to elicit a significant anti-tumor immune response. This is because, although autoreactive effector T cells (Teff) are present in the periphery of virtually all the subjects, they are kept in check by regulatory T cells (Treg) (2). Therefore, the balance between the number and/or the function of Teff and Treg appears to be highly crucial for the outcome of anti-tumor immunotherapy. In other words, an effective anti-tumor immune response can be obtained not only by enhancing Teff function but also by attenuating the suppressor function of Treg.

Among the different types of Treg identified so far, $CD4^+CD25^+$ Treg have been evaluated most extensively. It has become increasingly clear that Treg play a critical role in autoimmunity, transplantation and also in tumor immunity (3). Thus *in vivo* depletion of $CD4^+CD25^+$ Treg with anti-CD25 monoclonal antibody (PC61) has been shown to eradicate some but not all tumors in animal models (4-9). Additionally, our recent study has demonstrated that low-dose cyclophosphamide (20 mg/kg) also depletes Treg selectively and induced a significant anti-tumor immune response in a murine hepatoma cell line MH129 (10).

Glucocorticoid-induced tumor necrosis factor receptor (TNFR)-related protein (GITR), a member of the TNFR superfamily, is highly expressed in Treg (11). Although GITR expression is dispensable for Treg function (12), agonistic monoclonal antibody against GITR (DTA-1) has previously been shown to abrogate the suppressor function of Treg and consequently enhance the immune response (13,14). Therefore GITR was originally considered a potential target for

suppression of Treg function. Later, however, it was discovered that GITR is also expressed in resting $CD4^+CD25^-$ and $CD8^+$ T cells at low levels and was up-regulated upon activation, and the signal through GITR co-stimulated both $CD4^+CD25^-$ and $CD8^+$ T cells particularly with suboptimal T cell receptor stimulation (12,15). Importantly, the co-culture experiments with $CD4^+CD25^-$ and $CD4^+CD25^+$ T cells from wild-type or GITR knockout mice revealed that ligation of GITR on Teff is required to abrogate suppression by Treg (16). Thus it is currently believed that the signal through GITR mainly activates Teff rather than suppressing Treg (11,17).

In this study we evaluated the relative therapeutic efficacy of enhancement of Teff function through GITR signaling by adenovirus-mediated expression of GITR ligand (GITRL) and inhibition of suppressor function of Treg by depletion with PC61 or low-dose cyclophosphamide in two murine hepatoma cell lines, MH129 and MH134, of a similar origin.

Materials and methods

Cell lines and mice used. MH129 and MH134 cells were CCl_4-induced murine hepatoma cell lines from C3H/He strain (18), and were maintained in RPMI-1640 medium with 10% FCS and appropriate antibiotics. *In vitro* growth of each cell line was evaluated with the trypan blue exclusion test.

Six-week-old female C3H/HeN mice were purchased from Charles River (Tokyo, Japan) and kept in a specific pathogen-free facility. All experiments were conducted in accordance with the principles and procedures outlined in the Guideline for the Care and Use of Laboratory Animals in Nagasaki University.

Preparation of anti-CD25 monoclonal antibody. Anti-CD25 monoclonal antibody was purified from ascites of nude mice intraperitoneally injected with hybridoma PC61 using HiTrap™ protein G HP column (Amersham, Piscataway, NJ, USA). PC61 hybridoma was from Dr K. Yui, Nagasaki University, Nagasaki, Japan.

Construction of adenovirus expressing mouse GITRL. The plasmid containing cDNA for mouse GITRL (pTG16491) was kindly provided by Dr B. Calmels, Transgene, Strasburg, France (19). GITRL cDNA was excised by digestion with *Nhe*I and *Sal*I, and ligated into *Nhe*I- and *Sal*I-digested bicistronic vector pIRES2-AcGFP1 (Takara, Tokyo, Japan). The DNA fragment containing the GITRL cDNA, IRES and AcGFP was then released by *Nhe*I- and *Not*I-digestion and ligated into *Nhe*I- and *Not*I-digested adenovirus shuttle vector pHMCMV6 (20). The resulting plasmid pHM-GITRL-IRES-GFP was cut with *PI-Sce*I and *I-Ceu*I, and ligated into pAdHM15 (20). pAdHM-GITRL-IRES-GFP was linearized with *Pac*I, and transfected into 293 human embryonic kidney cells to yield Ad-GITRL-IRES-GFP. The adenovirus obtained was amplified in 293 cells and purified using two rounds of CsCl gradient centrifugation as previously described (21). Determination of plaque-forming unit (pfu) was also performed as previously described (21).

Expression of GITRL and GFP was confirmed by FACScan flow cytometry and Cell Quest software program (BD Biosciences, Mountain View, CA, USA) after staining the MH129 cells infected with Ad-GITRL-IRES-GFP at an MOI of 100 with PE-conjugated anti-GITRL antibody (e-Bioscience, San Diego, CA, USA).

Infectivity of MH129 and MH134 cells to adenovirus infection. The cells were infected with Ad-EGFP (a kind gift from Dr H. Yamasaki, Nagasaki University) at MOIs of 30, 100 and 300. On the next day, expression of EGFP was determined by flow cytometry as described above.

Expression of GITR on MH129 and MH134 cells. Expression of GITR on the cells was analyzed by staining the cells with PE-anti-GITR antibody (e-Bioscience) as described above.

In vivo experiments. The cells ($5x10^5$ cells/mouse) were subcutaneously injected into the flanks of mice. Tumor sizes were determined from caliper measurement using the standard formula (length x width^2/2) and expressed as the mean ± SE.

In the first series of experiments with cyclophosphamide and PC61, groups of mice were treated with either an intraperitoneal injection of cyclophosphamide (20 or 200 mg/kg) (Sigma-Aldrich, St. Louis, MO, USA) or PC61 (500 μg/mouse) four days before or after tumor cell inoculation. *In vivo* depletion of $CD25^+$ cells by PC61 was confirmed by flow cytometric analysis as described above after staining splenocytes four days after an intraperitoneal injection of antibody with FITC-conjugated-anti-CD4 and PE-anti-CD25 antibodies that recognize a different epitope of CD25 (7D4) (e-Bioscience) (10).

In the second series of experiments with GITRL, groups of mice were injected with the cells infected with Ad-GITRL-IRES-GFP or Ad-EGFP at an MOI of 100 for 24 h. Alternatively, other groups of mice were first injected with uninfected tumor cells, and when tumor sizes reached ~5 mm in diameter, $5x10^8$ pfu Ad-GITRL-IRES-GFP or Ad-EGFP in 50 μl PBS was injected intratumorally.

Finally, the combined effect of PC61 and Ad-GITRL-IRES-GFP was also studied. Groups of mice were injected on day 0 with the cells infected with Ad-GITRL-IRES-GFP at an MOI of 100 for 24 h, and were injected with PC61 on day +4 (MH129) or day -4 (MH134).

Results

As evident from our recent report (10) and Figs. 1 and 2 in this study, MH129 cells are susceptible to depletion of $CD25^+$ cells. Thus, injection of PC61 prevented tumor formation completely or partially when administered four days before or after tumor cell inoculation, respectively (Fig. 1A). $CD4^+CD25^+$ T cell depletion by low-dose cyclophosphamide (20 mg/kg) also significantly suppressed tumor growth (Fig. 2A). In contrast, MH134 cells were resistant to depletion of $CD25^+$ cells. As shown in Fig. 1B, injection of PC61 prior to tumor cell inoculation only partially delayed tumor growth, and injection following tumor cell inoculation contributed no effect. Low-dose cyclophosphamide also showed no significant therapeutic benefit (Fig. 2B). As we have recently demonstrated (10) and illustrated in Fig. 2, high-dose

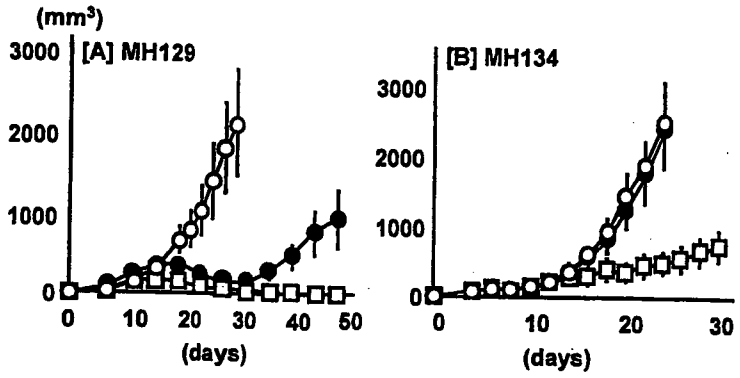

Figure 1. Anti-tumor effect of PC61 on MH129 and MH134 tumor cells in C3H/HeN mice. The mice were inoculated with $5x10^5$ MH129 (A) or MH134 (B) cells on day 0. Groups of mice were untreated (○) or treated with 500 μg PC61 on day -4 (□) or +4 (●). The data are the means ± SE (n=6). The same experiments were repeated at least twice with similar results.

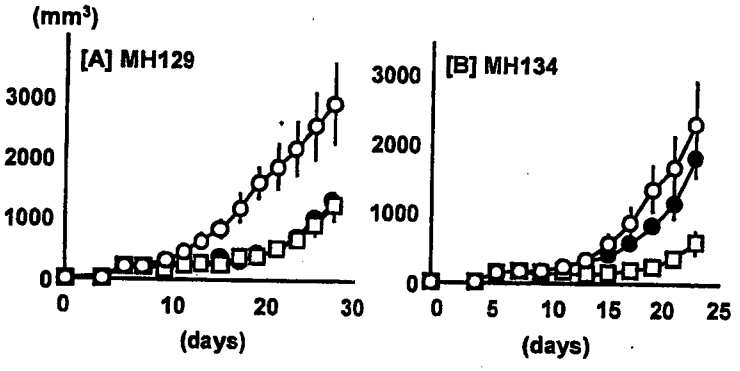

Figure 2. The anti-tumor effect of low (20 mg/kg)- and high (200 mg/kg)-dose cyclophosphamide on MH129 and MH134 tumor cells in C3H/HeN mice. The mice were inoculated with $5x10^5$ MH129 (A) or MH134 (B) cells on day 0. Groups of mice were untreated (○) or treated with high-dose (□) or low-dose (●) cyclophosphamide on day +4. The data are the means ± SE (n=6). The same experiments were repeated at least twice with similar results.

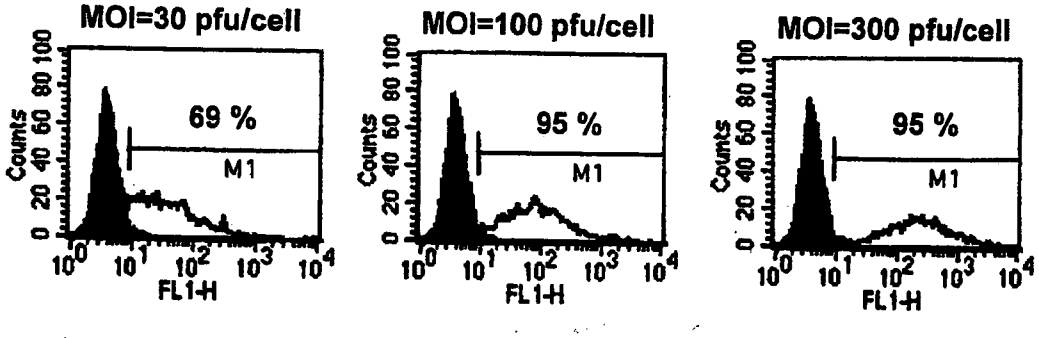

Figure 3. Flow cytometric analysis of MH129 cells infected with Ad-GITRL-IRES-GFP. The cells were untreated or infected with Ad-GITRL-IRES-GFP at an MOI of 100 pfu/cell. One day later, expression of GITRL and GFP was examined as described in Materials and methods.

cyclophosphamide was equally effective in both cell lines through its direct cytotoxic effect.

Since this difference, despite the similar origin of the two cell lines, may be attributed to different kinetics of peripheral $CD4^+CD25^+$ T cells in the two tumor models, the percentages of T cell subpopulations in splenocytes were studied. The ratios of $CD4^+CD25^+$ to $CD4^+$ T cells in the spleen remained unchanged during the experimental course (8.7±3.3% in the control; 9.2±1.2% in MH129-bearing mice at day 7, 6.2±2.5% in MH129-bearing mice at day 21; 7.2±1.9% in MH134-bearing mice at day 7; and 8.44±0.72% in MH134-bearing mice at day 21; mean ± SD).

The relative therapeutic effect of GITRL enhancement of Teff function in the two cell lines was next compared. To do this, recombinant, bicistronic adenovirus expressing GITRL and GFP was constructed. Expression of both molecules was confirmed by flow cytometry (Fig. 3). Ninety-five percent infectivity was observed at an MOI of 100 (Fig. 4). *In vitro* cell growth rates of both cells were not affected by infection with Ad-GITRL-IRES-GFP, and neither cells expressed GITR (data not shown). The *in vivo* effect of GITRL expression was evaluated by two different methods; one was by inoculation of adenoviral infected cells, and the other by injection of adenovirus into established tumors.

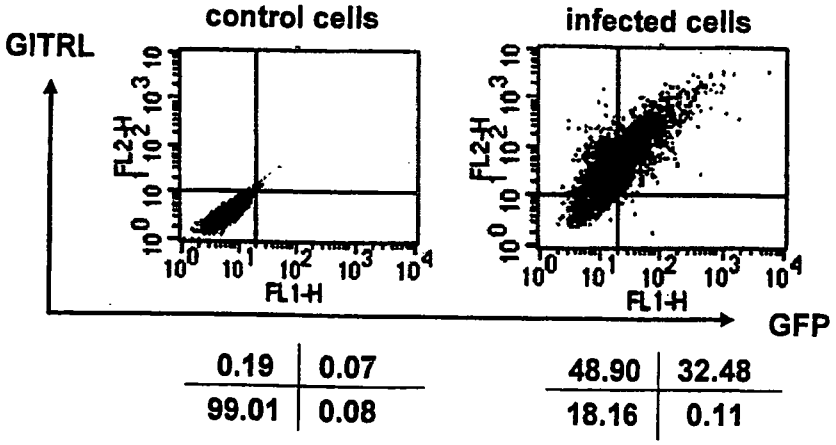

Figure 4. Flow cytometric analysis of adenovirus infectivity in MH129 cells. The cells were infected with Ad-EGFP at MOIs of 30, 100 and 300 pfu/cell. One day later, expression of EGFP was examined as described in Materials and methods.

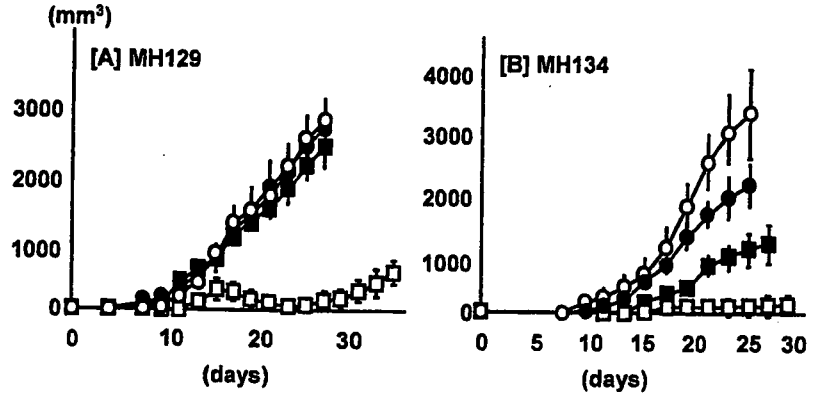

Figure 5. The anti-tumor effect of Ad-GITRL-IRES-GFP on MH129 and MH134 tumor cells in C3H/HeN mice. The mice were inoculated with $5x10^5$ MH129 (A) or MH134 (B) cells infected for 24 h with Ad-EGFP (○) or Ad-GITRL-IRES-GFP (■) on day 0. Alternatively the mice were inoculated with $5x10^5$ uninfected cells, and $5x10^8$ pfu Ad-EGFP (data not shown) or Ad-GITRL-IRES-GFP (●) were injected intratumorally when tumors became ~5 mm in diameter. Furthermore, the mice were also inoculated with Ad-GITRL-IRES-GFP-infected cells and treated with PC61 four days after or before tumor cell inoculation in the MH129 and MH134 cells, respectively (□). The data are the means ± SE (n=6-12). The same experiments were repeated at least twice with similar results.

In vivo growth of MH129 tumors was not affected by GITRL expression for either method (Fig. 5A). However, MH134 tumor growth was blunted by GITRL, particularly when the cells were infected with Ad-GITRL-IRES-GFP before inoculation (Fig. 5B). Thus, the relative responses of two hepatoma cell lines to Treg depletion and Teff enhancement are quite different; MH129 cells are susceptible to the former but resistant to the latter, and *vice versa* for MH134 cells.

Finally, the combined effect of PC61 and GITRL was also studied. The tumor cells were infected with Ad-GITRL-IRES-GFP prior to tumor cell inoculation, and PC61 was injected four days after or before tumor cell inoculation in MH129 and MH134, respectively. The additive effect of PC61 and GITRL was observed only in MH134 cells ($p<0.05$, Figs. 1 and 5) in the combination study.

Discussion

Effective therapeutic outcome of anti-tumor immunotherapy may be obtained by attenuating Treg suppressor function and/or enhancing Teff, for example, by depletion of Treg with PC61 or low-dose cyclophosphamide and stimulation of Teff by GITR signal or DTA-1, respectively. The therapeutic efficacies of PC61 and GITRL or DTA-1, alone or in combination with other antigen-specific immunotherapies, have recently been documented in animal models, showing that the effects of PC61 and DTA-1 vary in different types of tumor cells. For example, Meth A fibrosarcoma cells are sensitive but B16 melanoma cells are resistant to both antibodies (4,5,17,22,23). Thus it is generally accepted that Treg depletion and Teff enhancement can increase antitumor immunity against highly immunogenic tumors but has little or no effect against poorly to non-immunogenic tumors (17). However our present study clearly shows that the relative responsiveness to GITRL and PC61 is different even in two murine hepatoma cells of a similar origin.

The exact mechanism(s) of this difference are at present unclear, but may not be explained by a difference in immunogenicity of these cells, because each tumor cell line responded to at least one therapeutic approach. Also a different kinetics of peripheral Treg between these tumor models is also unlikely, because there was no difference in peripheral Treg number between these models. Instead, a difference in relative induction levels of Teff versus Treg by each cell line

may explicate our results. From our results we suggest the following scenario. It is clear that the balance between Teff and Treg tipped toward Treg in these two tumor models, because both tumors grew well in syngeneic immunocompetent mice. However, MH129 tumor cells substantially activated both Teff and Treg (but Treg > Teff). The depletion of Treg could reverse this balance, thereby leading to tumor shrinkage; however, Teff were already activated fully and GITRL was therefore ineffective. In contrast, the activation of Treg was considerably high, but that of Teff trifling in MH134 cells. The depletion of Treg by PC61 could therefore not enhance tumor immunity because of negligible Teff activity; while activated Teff by GITRL overweighed Treg and enhanced anti-tumor immunity. In these cases, activation of Treg does not necessarily mean proliferation of Treg, because the number of $CD4^+CD25^+$ Treg was unaltered after tumor cell inoculation in our study. An additive effect of PC61 and GITR in MH134 cells, not in MH129, fits our hypothesis.

Notably, a recent study has shown that tumor antigen(s) prime both Teff and Treg even in the same regional lymph nodes (24), and moreover another study has also shown that certain antigen(s) selectively induce Treg (25).

To confirm our hypothesis, future studies identifying tumor antigen(s) or epitope(s) specific for Teff and Treg in these tumor cells will be required. Analysis of immune response to such antigen(s) or epitope(s) may help predict the relative efficacy of different immunotherapies against distinct tumors.

References

1. Houghton AN and Guevara-Patino JA: Immune recognition of self in immunity against cancer. J Clin Invest 114: 468-471, 2004.
2. Danke NA, Koelle DM, Yee C, Beheray S and Kwok WW: Autoreactive T cells in healthy individuals. J Immunol 172: 5967-5972, 2004.
3. Sakaguchi S: Naturally rising Foxp3-expressing $CD4^+CD25^+$ regulatory T cells in immunological tolerance to self and non-self. Nat Immunol 6: 345-352, 2005.
4. Shimizu J, Yamasaki S and Sakaguchi S: Induction of tumor immunity by removing $CD25^+CD4^+$ T cells: a common basis between tumor immunity and autoimmunity. J Immunol 163: 5211-5218, 1999.
5. Onizuka S, Tawara I, Shimizu J, Sakaguchi S, Fujita T and Nakayama E: Tumor rejection by *in vivo* administration of anti-CD25 (interleukin-2 receptor α) monoclonal antibody. Cancer Res 59: 3128-3133, 1999.
6. Tanaka H, Tanaka J, Kjaergaard J and Shu S: Depletion of $CD4^+CD25^+$ regulatory cells augments the generation of specific immune T cells in tumor-draining lymph nodes. J Immunother 25: 207-217, 2002.
7. Jones E, Dahm-Vicker M, Simon AK, Green A, Powrie F, Cerundolo V and Gallimore A: Depletion of $CD25^+$ regulatory cells results in suppression of melanoma growth and induction of autoreactivity in mice. Cancer Immun 2: 1, 2002.
8. Golgher D, Jones E, Powrie F, Elliot T and Gallimore A: Depletion of $CD25^+$ regulatory cells uncovers immune responses to shared murine tumor rejection. Eur J Immunol 32: 3267-3275, 2002.
9. Sutmuller RP, van Duivenvoorde LM, van Elsas A, Schumacher TN, Wildenberg ME, Allison JP, Toes RE, Offringa R and Melief CJ: Synergism of cytotoxic T lymphocytes-associated antigen 4 blockade and depletion of $CD25^+$ regulatory T cells in antitumor therapy reveals alternative pathways for suppression of autoreactive cytotoxic T lymphocyte responses. J Exp Med 194: 823-832, 2001.
10. Motoyoshi Y, Kaminoda K, Saitoh O, Hamasaki K, Nakao K, Ishii N, Nagayama Y and Eguchi K: Different mechanisms for anti-tumor effects of low- and high-dose cyclophosphamide. Oncol Rep 16: 141-146, 2006.
11. Shevach EM and Stephens GL: The GITR-GITRL interaction: co-stimulation or contrasuppression of regulatory activity? Nat Rev Immunol 6: 613-618, 2006.
12. Ronchetti S, Zollo O, Bruscoli S, Agostini M, Bianchiri R, Nocentini G, Ayroldi E and Riccadi C: GITR, a member of the TNF receptor superfamily is costimulatory to mouse T lymphocyte subpopulations. Eur J Immunol 34: 613-622, 2004.
13. Shimizu J, Yamasaki S, Takahashi T, Ishida Y and Sakaguchi S: Stimulation of $CD25^+CD4^+$ regulatory T cells through GITR breaks immunological self-tolerance. Nat Immunol 3: 135-142, 2002.
14. McHugh R, Whitters MJ, Piccirillo CA, Young DA, Shevach EM, Collins M and Byrne MC: $CD4^+CD25^+$ immunoregulatory T cells: gene expression analysis reveals a functional role for the glucocorticoid-induced TNF receptor. Immunity 16: 311-323, 2002.
15. Kanamaru F, Youngnak P, Hashiguchi M, Nishioka T, Takahashi T, Sakaguchi S, Ishikawa I and Azuma M: Costimulation via glucocorticoid-induced TNF receptor in both conventional and $CD25^+$ regulatory $CD4^+$ T cells. J Immunol 172: 7306-7314, 2004.
16. Stephens GL, McHugh RS, Whitters MJ, Young DA, Luxenberg D, Carreno BM, Collins M and Shevach EM: Engagement of glucocorticoid-induced TNFR family-related receptor on effector T cells by its ligand mediates resistance to suppression by $CD4^+CD25^+$ T cells. J Immunol 173: 5008-5020, 2004.
17. Ramirez-Montagut T, Chow A, Hirschhorn-Cymerman D, Terwey TH, Kochman AA, Lu S, Miles RC, Sakaguchi S, Houghton AN and van den Brink MRM: Glucocorticoid-induced TNF receptor family related gene activation overcomes tolerance/ignorance to melanoma differentiation antigens and enhances antitumor immunity. J Immunol 176: 6434-6442, 2006.
18. Shima J, Yoshioka T, Kosugi A, Ogata M, Fujiwara H and Hamaoka T: Differential ability of tumor-unique and cross-reactive antigen(s) on two murine hepatoma cell lines to induce $Lyt\text{-}1^+2^-$ T cells responsible for *in vivo* protective immunity. BIKEN J 30: 1-8, 1987.
19. Calmels B, Paul S, Futin N, Ledoux C, Stoeckel F and Acres B: Bypassing tumor-associated immune suppression with recombinant adenovirus expressing membrane bound or secreted GITR-L. Cancer Gene Ther 12: 198-205, 2005.
20. Mizuguchi H, Koizumi N, Hosono T, Utoguchi N, Watanabe Y, Kay MA and Hayakawa T: A simplified system for constructing recombinant adenoviral vectors containing heterologous peptides in the HI loop of their fiber knob. Gene Ther 8: 730-735, 2001.
21. Nagayama Y, Nishihara E, Namba H, Yokoi H, Hasegawa M, Mizuguchi H, Hayakawa T, Yamashita S and Niwa M: Targeting the replication of adenovirus to *p53*-defective thyroid carcinoma with a *p53*-regulated Cre-*lox*P system. Cancer Gene Ther 8: 36-44, 2001.
22. Ko K, Yamasaki S, Nakayama K, Nishioka T, Hirota K, Yamaguchi T, Shimizu J, Nomura T, Chiba T and Sakaguchi S: Treatment of advanced tumors with agonistic anti-GITR mAb and its effects on tumor-infiltrating $Foxp3^+CD25^+CD4^+$ regulatory T cells. J Exp Med 202: 885-891, 2005.
23. Cohen AD, Diab A, Perales MA, Wolchok JD, Rizzuto G, Merghoub T, Huggins D, Liu C, Turk MJ, Restifo NP, Sakaguchi S and Houghton AN: Agonist anti-GITR antibody enhances vaccine-induced $CD8^+$ T-cell responses and tumor immunity. Cancer Res 66: 4902-4912, 2006.
24. Hiura T, Kagamu H, Miura S, Ishida A, Tanaka H, Tanaka J, Gejyo F and Yoshizawa H: Both regulatory T cells and antitumor effector T cells are primed in the same draining lymph nodes during tumor progression. J Immunol 175: 5058-5066, 2005.
25. Nishikawa H, Kato T, Tanida K, Hiasa A, Tawara I, Ikeda H, Ikarashi Y, Wakasugi H, Kronenberg M, Nakayama T, Taniguchi M, Kuribayashi K, Old LJ and Shiku H: $CD4^+$ $CD25^+$ T cells responding to serologically defined autoantigens suppress antitumor immune responses. Proc Natl Acad Sci USA 100: 10902-10906, 2003.

Online Submissions: wjg.wjgnet.com
www.wjgnet.com
wjg@wjgnet.com

World J Gastroenterol 2007 August 14; 13(30): 4149-4151
World Journal of Gastroenterology ISSN 1007-9327

CASE REPORT

Clearance of hepatitis C virus after living-donor liver transplantation in spite of residual viremia on end date of interferon therapy before transplantation

Tatsuki Ichikawa, Kazuhiko Nakao, Keisuke Hamasaki, Takuya Honda, Hidetaka Shibata, Mana Akahoshi, Susumu Eguchi, Mitsuhisa Takatsuki, Takashi Kanematsu, Katsumi Eguchi

Tatsuki Ichikawa, Kazuhiko Nakao, Keisuke Hamasaki, Takuya Honda, Hidetaka Shibata, Mana Akahoshi, Katsumi Eguchi, The First Department of Internal Medicine, Graduate School of Biomedical Science, Nagasaki University, Nagasaki 852-8501, Japan
Susumu Eguchi, Mitsuhisa Takatsuki, Takashi Kanematsu, Department of Transplantation and Digestive Surgery, Graduate School of Biomedical Science, Nagasaki University, Nagasaki 852-8501, Japan
Correspondence to: Tatsuki Ichikawa, MD, The First Department of Internal Medicine, Graduate School of Biomedical Science, Nagasaki University, 1-7-1 Sakamoto, Nagasaki 852-8501, Japan. ichikawa@net.nagasaki-u.ac.jp
Telephone: +81-95-8497260 Fax: +81-95-8497270
Received: 2007-04-14 Accepted: 2007-05-12

Abstract

Interferon (IFN) therapy is the only treatment strategy for hepatitis C virus (HCV) infection after liver transplantation (LT), but prophylactic and treatable IFN therapy after LT has been shown to be insufficient due to the adverse effects of IFN and rivabirin. In this paper, we describe the disappearance of HCV after LT without IFN therapy in the presence of residual viremia on the day of LT. We herein report our findings since this is considered an important case for the anti-HCV strategy of post LT. A 60-year old woman with LC and HCC was referred to Nagasaki University Hospital in August 2004. After she underwent LT on February 18, 2005, we injected peg-IFN-α-2a the 11th time at 18 wk and HCV-RNA was still positive in the serum at LT. The serum HCV-RNA was negative one month after operation and subsequently dissolved 15 mo after operation without IFN therapy. As a result, we speculate that if HCV-RNA is positive while HCV core antigen is negative before LT, then it may lead to clearance of HCV after LT. Therefore long acting peg-IFN-α-2a is thus considered a potentially effective agent for the treatment of HCV-related cirrhosis before LT.

Key words: Pegylated interferon; Liver transplantation; Hepatitis C virus

Ichikawa T, Nakao K, Hamasaki K, Honda T, Shibata H, Akahoshi M, Eguchi S, Takatsuki M, Kanematsu T, Eguchi K. Clearance of hepatitis C virus after living-donor liver transplantation in spite of residual viremia on end date of interferon therapy before transplantation. *World J Gastroenterol* 2007; 13(30): 4149-4151

http://www.wjgnet.com/1007-9327/13/4149.asp

INTRODUCTION

Living donor liver transplantation (LDLT) has become a common treatment strategy for hepatocellular carcinoma (HCC) and end stage liver cirrhosis (LC) in Japan[1]. However, hepatitis C virus (HCV) infection, the most common cause of LDLT, is found in nearly all re-infected graft livers, thus leading to a rapid progression to LC and re-liver transplantation[2]. Interferon (IFN) treatment for HCV infection after LT is the only treatment strategy at present, but its effects are still incomplete[3]. Because the titer of HCV is the most decay in early transplant phase of liver transplantation[4], anti-HCV therapy could thus be considered at this time[5], but prophylactic and treatable IFN therapy after LT has so far been ineffective due to the adverse effects of IFN and rivabirin[6].

Recently, pegylated interferon (peg-IFN), utilizing polyethyleneglycol moiety attached to IFN *via* an amide bond, has been used in the treatment of chronic HCV infection. Peg-IFN-α-2a characterized by a prolonged absorption half-life (50 h), a restricted volume of distribution (8-12 L), and a decreased clearance (94 mL/h)[7], has been found to be safe and tolerable after LT[8]. We thus consider peg-IFN-α-2a a potentially useful treatment of LC due to HCV infection in patients awaiting liver transplantation.

In this case, we made an attempt to achieve HCV clearance from a graft liver after LDLT. For this purpose, peg-IFN-α-2a mono-therapy was performed for 13 wk until LDLT. We observed the disappearance of HCV after LDLT without IFN therapy in the presence of residual viremia on the day of LDLT. The titer of HCV disappeared in early post-LDLT due to the administration of peg-IFN-α-2a. We herein report our findings.

CASE REPORT

A 60-year old woman with LC and HCC was referred

to Nagasaki University Hospital in August 2004. She was diagnosed having diabetes and HCV-related LC in 1995 and 1999, respectively, and had no history of blood transfusion, alcohol abuse and intra-venous drug use. After the diagnosis of LC, she was treated with IFN-α, but this medication was stopped due to depression. In August 2003, a tumor was detected measuring 3.5 cm in diameter in the caudate lobe of the liver, she underwent trans-arterial chemoembolization (TACE) therapy twice in September 2003 and February 2004. The HCC decreased and no new HCC was detected. However, she suffered from hepatic encephalopathy (disorientation and flapping tremor) in June 2004 and thus was hospitalized. Consequently she and her family decided to undergo living donor liver transplantation at our hospital.

She entered our hospital for evaluation of LDLT in September 2004 (Figure 1). On admission, she had no ascites or hepatic encephalopathy. Laboratory data revealed 2.0 mg/dL total bilirubin, 97 IU/L AST, 88 IU/L ALT, 855 IU/L ALP, 6.7 mg/dL total protein, 3.1 mg/dL albumin, 76% prothrombin time and 81000/μL platelets, she was thus evaluated to be Child-Pugh grade B. Her HCV genotype was 1b, and the viral load in serum was 1860 KIU/mL by Amplicor PCR or 3320 fmol/L by HCV core antigen assay. HCC remained unchanged on admission. She underwent peg-IFN-α-2a treatment with the goal of virus clearance, because LDLT might be unnecessary depending on the status of her liver function. We concluded that LDLT should be performed after disappearance of HCV-RNA in her serum. She received peg-IFN-α-2a, 90 μg once a week from December 12, but we had to discontinue it due to neutropenia (under 500/μL) after the first week of therapy. As a result, we modified the regimen of peg-IFN-α-2a treatment from once a week to once every two weeks.

At five weeks after initiation of peg-IFN-α-2a treatment, HCV core antigen was not detectable in her serum, but HCV-RNA was still detectable by qualitative PCR(nested PCR) even at 12 wk after initiation of therapy. We therefore decided to perform LDLT with her daughter as donor, since the complete disappearance of HCV-RNA was thought to be impossible. She underwent LDLT on February 18, 2005, and we used peg-IFN-α-2a for the 11th time at 18 wk and HCV-RNA was still positive in the serum at this time.

Surgery was successfully performed. Histopathological examination revealed that the explanted liver exhibited mixed macro and micro nodular cirrhosis, and three tumors were observed in the caudate lobe, one of them showed complete necrosis by TACE while the others were viable and diagnosed with well-differentiated HCC, and another well-differentiated HCC was found in the anterior segment of the explanted liver. There was no-evidence of vascular invasion of HCC. The patient was given tacrolimus and predonisolone as immunosuppressants. On postoperative day (POD) 2, she underwent re-anastomosis of the hepatic artery, because of decreased arterial flow caused by an intimal tear. On POD 5, she underwent the third laparotomy, because of hematoma around the portal vein and thrombosis in the portal vein. Due to food aspiration, methicillin resistance staphylococcus aureus (MRSA) caused pneumonia and a systemic infection. At this time, icterus was worsening and the total bilirubin in serum rose to 30 mg/dL on POD 30. She was treated with intensive care, tracheostomy, artificial respiration, MRSA specific antibiotics, hyperbaric oxygen therapy and steroid pulse therapy. Finally, at post operative month (POM) 4, she was weaned off artificial respiration and her total bililubin decreased to 3.1 mg/dL and she showed a good recovery at POM 8. At POM 13, she was operated on for anastomotic stricture of the common bile duct and was then treated on an out-patient basis.

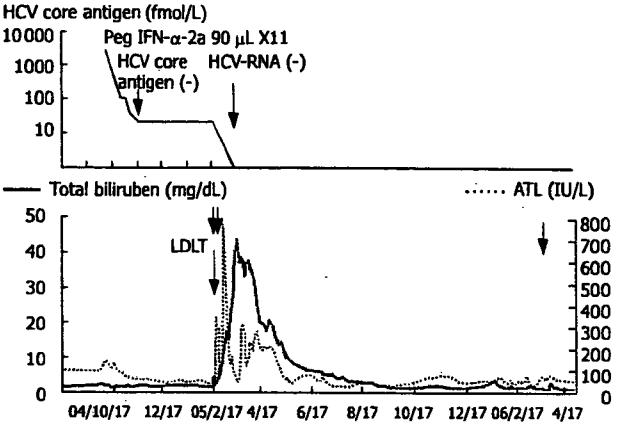

Figure 1 Clinical course of the disease at our hospital. The upper diagram showing the course of the virus titter, in which HCV is the core antigen (fmol/L), and expediently negative HCV core antigen is denoted as 20 fmol/L and negative qualitative HCV-RNA as 1 fmol/L. The lower diagram showing the course of total bilirubin and AST. Three small arrows show abdominal operation after LDLT and a large arrow demonstrates LDLT.

Serum HCV-RNA was negative at POM 1 and subsequently dissolved at POM 15. Liver biopsies performed at POD 2, 5, 32 and POM 13 revealed no findings of HCV reactivation.

DISCUSSION

Crippin JS and colleagues[9] tried IFN-α-2b (1 or 3 MU/d three time a week) +/- ribavirin (400 mg) within 12 weeks, and a loss of detectable HCV-RNA was seen in 5/15 (33%) patients. Thomas RM and colleagues[10] reported that 12 cases (60%) responded to IFN-α-2b 5 MU/d therapy before LT with a clearance of serum HCV-RNA, four of the 12 cases did not show any evidence of HCV recurrence after LD. Forns X and colleagues[11] used IFN-α-2b 3 MU/d + ribavirin 800 mg/d and 9 cases (30%) demonstrated a clearance of serum HCV-RNA, 6 of the 9 cases did not have any evidence of HCV recurrence after LD. Recently, Everson GT and colleagues[12] described that low dose IFN treatment, peg-IFN-α-2b 0.5 μg/kg per week or IFN-α-2b 1.5 MU/d + ribavirin 600 mg/d per six months for genotypes 2 and 3 or 1 year for genotype 1, was performed for advanced HCV patients, and 12 of 15 cases showing a clearance of HCV-RNA before LT remained HCV-RNA negative 6 or more months after transplantation and 32 cases who were positive for HCV-RNA before remained HCV-RNA positive. In a previous report[13], IFN therapy before LT was shown

to be an effective treatment for the clearance of HCV with advanced LC, but sustained HCV clearance after LT was never acquired in patients with a detectable level of HCV before LT. In contrast, our case demonstrated a clearance of HCV-RNA regardless of the fact that HCV-RNA in serum was positive before LDLT. After liver transplantation, we did not prescribe cyclosporine A and mycophenorate mofetil exerting anti-HCV effects *in vitro*. We hypothesize that peg-IFN-α-2a as a long acting IFN, when injected immediately prior to LDLT, may thus induce an anti-viral activity in the anhepatic phase and also soon after LDLT. The HCV titer is the lowest in the anhepatic phase and the immediately early post LDLT[4], therefore this period requires treatment in order to achieve a clearance of HCV. In our case, HCV showed trace quantities due to the negative HCV core antigen and positive HCV-RNA. We thus speculate that trace quantities of HCV in the graft respond to the continuing presence of peg-IFN-α-2a, though a similar case has not been reported up to now.

In cases of a sustained viral response to IFN therapy after LT, hepatic fibrosis does not progress except for other reasons of hepatic injury, rejection and stenosis of bile[14,15]. HCV relapse post SVR after LT has been reported at 7, 8 and 15 mo after treatment[15,16]. For the reasons stated above, we must pay attention to advanced liver fibrosis and HCV-RNA in the serum.

Based on our findings, we hypothesize that positive HCV-RNA is positive and negative HCV core antigen before LT may lead to a clearance of HCV after LT, and long acting peg-IFN-α-2a may be a potentially effective agent for HCV infection before LT. This hypothesis should be further confirmed.

REFERENCES

1 **Takada Y**, Ueda M, Ito T, Sakamoto S, Haga H, Maetani Y, Ogawa K, Kasahara M, Oike F, Egawa H, Tanaka K. Living donor liver transplantation as a second-line therapeutic strategy for patients with hepatocellular carcinoma. *Liver Transpl* 2006; **12**: 912-919

2 **Berenguer M**, Ferrell L, Watson J, Prieto M, Kim M, Rayon M, Cordoba J, Herola A, Ascher N, Mir J, Berenguer J, Wright TL. HCV-related fibrosis progression following liver transplantation: increase in recent years. *J Hepatol* 2000; **32**: 673-684

3 **Terrault NA**. Prophylactic and preemptive therapies for hepatitis C virus-infected patients undergoing liver transplantation. *Liver Transpl* 2003; 9: S95-S100

4 **Garcia-Retortillo M**, Forns X, Feliu A, Moitinho E, Costa J, Navasa M, Rimola A, Rodes J. Hepatitis C virus kinetics during and immediately after liver transplantation. *Hepatology* 2002; **35**: 680-687

5 **Powers KA**, Ribeiro RM, Patel K, Pianko S, Nyberg L, Pockros P, Conrad AJ, McHutchison J, Perelson AS. Kinetics of hepatitis C virus reinfection after liver transplantation. *Liver Transpl* 2006; **12**: 207-216

6 **Shergill AK**, Khalili M, Straley S, Bollinger K, Roberts JP, Ascher NA, Terrault NA. Applicability, tolerability and efficacy of preemptive antiviral therapy in hepatitis C-infected patients undergoing liver transplantation. *Am J Transplant* 2005; **5**: 118-124

7 **Bruno R**, Sacchi P, Ciappina V, Zochetti C, Patruno S, Maiocchi L, Filice G. Viral dynamics and pharmacokinetics of peginterferon alpha-2a and peginterferon alpha-2b in naive patients with chronic hepatitis c: a randomized, controlled study. *Antivir Ther* 2004; **9**: 491-497

8 **Chalasani N**, Manzarbeitia C, Ferenci P, Vogel W, Fontana RJ, Voigt M, Riely C, Martin P, Teperman L, Jiao J, Lopez-Talavera JC. Peginterferon alfa-2a for hepatitis C after liver transplantation: two randomized, controlled trials. *Hepatology* 2005; **41**: 289-298

9 **Crippin JS**, McCashland T, Terrault N, Sheiner P, Charlton MR. A pilot study of the tolerability and efficacy of antiviral therapy in hepatitis C virus-infected patients awaiting liver transplantation. *Liver Transpl* 2002; **8**: 350-855

10 **Thomas RM**, Brems JJ, Guzman-Hartman G, Yong S, Cavaliere P, Van Thiel DH. Infection with chronic hepatitis C virus and liver transplantation: a role for interferon therapy before transplantation. *Liver Transpl* 2003; **9**: 905-915

11 **Forns X**, Garcia-Retortillo M, Serrano T, Feliu A, Suarez F, de la Mata M, Garcia-Valdecasas JC, Navasa M, Rimola A, Rodes J. Antiviral therapy of patients with decompensated cirrhosis to prevent recurrence of hepatitis C after liver transplantation. *J Hepatol* 2003; **39**: 389-396

12 **Everson GT**, Trotter J, Forman L, Kugelmas M, Halprin A, Fey B, Ray C. Treatment of advanced hepatitis C with a low accelerating dosage regimen of antiviral therapy. *Hepatology* 2005; **42**: 255-262

13 **Henry SD**, Metselaar HJ, Lonsdale RC, Kok A, Haagmans BL, Tilanus HW, van der Laan LJ. Mycophenolic acid inhibits hepatitis C virus replication and acts in synergy with cyclosporin A and interferon-alpha. *Gastroenterology* 2006; **131**: 1452-1462

14 **Abdelmalek MF**, Firpi RJ, Soldevila-Pico C, Reed AI, Hemming AW, Liu C, Crawford JM, Davis GL, Nelson DR. Sustained viral response to interferon and ribavirin in liver transplant recipients with recurrent hepatitis C. *Liver Transpl* 2004; **10**: 199-207

15 **Bizollon T**, Pradat P, Mabrut JY, Chevallier M, Adham M, Radenne S, Souquet JC, Ducerf C, Baulieux J, Zoulim F, Trepo C. Benefit of sustained virological response to combination therapy on graft survival of liver transplanted patients with recurrent chronic hepatitis C. *Am J Transplant* 2005; **5**: 1909-1913

16 **Bizollon T**, Ahmed SN, Radenne S, Chevallier M, Chevallier P, Parvaz P, Guichard S, Ducerf C, Baulieux J, Zoulim F, Trepo C. Long term histological improvement and clearance of intrahepatic hepatitis C virus RNA following sustained response to interferon-ribavirin combination therapy in liver transplanted patients with hepatitis C virus recurrence. *Gut* 2003; **52**: 283-287

S- Editor Liu Y **L- Editor** Wang XL **E- Editor** Liu Y

ELSEVIER

Journal of Hepatology 47 (2007) 546–555

Journal of Hepatology

www.elsevier.com/locate/jhep

Abrogation of constitutive STAT3 activity sensitizes human hepatoma cells to TRAIL-mediated apoptosis☆

Mariko Kusaba, Kazuhiko Nakao*, Takashi Goto, Daisuke Nishimura, Hiroshi Kawashimo, Hidetaka Shibata, Yasuhide Motoyoshi, Naota Taura, Tatsuki Ichikawa, Keisuke Hamasaki, Katsumi Eguchi

First Department of Internal Medicine, Nagasaki University School of Medicine, 1-7-1, Sakamoto, Nagasaki 852-8501, Japan

***Background/Aims*: Signal transducer and activator of transcription 3 (STAT3) is constitutively activated and regulates cell growth and survival of various cancer cells. We investigated the anti-tumor effect of AG490, a Janus kinase 2 specific inhibitor, in human hepatoma cells.**

***Methods*: Effects of AG490 on STAT3 activation, on cell-growth and survival, and on the expression of cell-cycle- and apoptosis-related proteins were evaluated in Huh-1, Huh-7, HepG2 and Hep3B cells. Next, whether AG490 renders hepatoma cells susceptible to tumor necrosis factor-related apoptosis-inducing ligand (TRAIL) was examined *in vitro* and *in vivo*.**

***Results*: Constitutively activated STAT3 through tyrosine phosphorylation was detected in all hepatoma cells. AG490 inhibited the phosphorylation of STAT3 and its activity. AG490 induced cell cycle arrest in Huh-1, Huh-7 and HepG2 through cyclin D1 downregulation, and induced marked apoptosis in Hep3B. AG490 downregulated at least one of the anti-apoptotic proteins, Bcl-xL, survivin or XIAP in all hepatoma cells. AG490 sensitized Huh-1, Huh-7 and HepG2 to TRAIL-induced apoptosis *in vitro*. Intraperitoneal injection of AG490, the combination of AG490 and TRAIL more greatly, repressed the growth of subcutaneous Huh-7 tumors in athymic mice.**

***Conclusions*: Abrogation of constitutive activation of STAT3 by AG490 enhances the anti-tumor activity of TRAIL against human hepatoma cells.**

***Keywords*: STAT3; AG490; TRAIL; Hepatoma**

1. Introduction

Signal transducer and activator of transcription (STAT) proteins become activated by tyrosine phosphorylation in response to cytokines and growth factors, which typically occurs through cytokine receptor-associated kinases, the Janus kinase (JAK) family proteins [1]. Recent studies have demonstrated that constitutively activated STAT signaling, especially STAT3, contributes to oncogenesis [2,3]. In fact, constitutive activation of STAT3 has been observed in various cancer cells [2–8], suggesting that STAT3 plays a crucial role in the regulation of cell proliferation and survival in cancer. Furthermore, abrogation of STAT3 signaling by

Received 1 December 2006; received in revised form 24 April 2007; accepted 26 April 2007; available online 6 June 2007
Associate Editor: K. Koike

☆ The authors who have taken part in this study declared that they have no relationship with the manufacturers of the materials involved either in the past or present and did not receive funding from the manufacturers to carry out their research. They did not receive funding from any source to carry out this study.

* Corresponding author. Tel.: +81 95 849 7261; fax: +81 95 849 7261.
E-mail address: kazuhiko@net.nagasaki-u.ac.jp (K. Nakao).

Abbreviations: JAK2, Janus kinase 2; SOCS, suppressor of cytokine signaling; STAT3, signal transducer and activator of transcription 3; TRAIL, tumor necrosis factor-related apoptosis-inducing ligand.

0168-8278/$32.00
doi:10.1016/j.jhep.2007.04.017

chemical inhibitors [9,10], a dominant negative STAT3 mutant [11,12], inhibitory phosphotyrosyl peptides [13], decoy oligonucleotides [14], antisense STAT3 oligonucleotides [15] has resulted in inhibition of cell proliferation and induction of apoptosis in various cancer cells [16].

Hepatitis B virus (HBV) and hepatitis C virus (HCV) are closely linked to the development of hepatocellular carcinoma (HCC) [17,18]. Recently, it has been reported that suppressor of cytokine signaling (SOCS)-1 and SOCS-3, negative regulators of the JAK2-STAT signaling pathway, are silenced by methylation in human hepatoma cell lines and HCC tissues, which leads to constitutive activation of STAT3 in these cells [19,20]. It was also reported that STATs including STAT3 were aberrantly activated in HCC tissues compared with surrounding normal liver tissues [21,22]. In addition, several studies have shown that HCV constitutively activates STAT3 through oxidative stress [23], and that the HCV core protein can activate STAT3, resulting in the cellular transformation [24]. Taken together, it is possible that the constitutive activation of STAT3 is involved in hepatocarcinogenesis.

Tumor necrosis factor (TNF)-related apoptosis-inducing ligand (TRAIL), a novel member of the TNF superfamily, is a promising candidate for cancer therapy since it preferentially induces apoptosis in various cancer cells with little or no effect on normal cells [25,26]. However, high concentrations of TRAIL are necessary to induce apoptosis in certain cancer cells, including human hepatoma cells [27]. Thus, combinations of TRAIL with several chemotherapeutic agents or radiation have been evaluated for rendering such cells susceptible to TRAIL, and some combinations have successfully enhanced TRAIL-mediated cancer cell death [27–29].

In the present study, we examined the status of STAT3 activation in human hepatoma cells and the effect of the JAK2 inhibitor, AG490, on STAT3 activation and on cell proliferation and survival. Furthermore, we have evaluated whether abrogation of STAT3 signaling by AG490 sensitizes hepatoma cells to TRAIL-induced apoptosis *in vitro* and combination of AG490 and TRAIL exhibits anti-tumor effect *in vivo*.

2. Materials and methods

2.1. Cell culture and reagents

The human hepatoma cell lines, Huh-1, HuH-7, HepG2 and Hep3B, were maintained in a chemically defined medium, IS-RPMI [30] containing 10% fetal bovine serum. Normal human hepatocytes (Hc cells) [31] were purchased from the Applied Cell Biology Research Institute (Kirkland, WA) and maintained in CS-C complete medium. A JAK-2 specific inhibitor, AG490, was purchased from Calbiochem (San Diego, CA). Recombinant human TRAIL was purchased from R&D systems (Minneapolis, MN). In some experiments, interleukin-6 (IL-6) (R&D systems), cell permeable STAT3 inhibitor peptide containing STAT3-SH2 domain-binding PY*LKTK where Y* represents phosphotyrosine (Calbiochem) [13], and DR4 and DR5-specific blocking chimera antibodies (DR4-chimera and DR5-chimera) (R&D systems) were added to the cell cultures.

2.2. Cell transfection and luciferase assay

The plasmids pTA-Luc (Clontech, Mountain View, CA) containing the minimal TA promoter and the firefly luciferase gene, pSTAT3-TA-Luc (Clontech), containing four copies of the binding sequence of STAT3 located upstream of pTA-Luc promoter, and pRL-CMV-Luc (Promega, Madison, WI) containing the CMV immediate early enhancer/promoter and the *Renilla* luciferase gene were used. Cells were grown in 24-well multiplates the day before transfection. Two hundred nanograms of pSTAT3-TA-Luc or pTA-Luc together with 10 ng pRL-CMV-Luc was transfected into the cells by the lipofection method. After 6 h incubation, the medium was replaced with fresh medium with or without IL-6 (20, 40 ng/ml), AG490 (25, 100 μM) or STAT3 inhibitor peptide (0.1, 0.5 mM), and the cells were incubated for 24 h. Luciferase activity was determined by a dual-luciferase reporter assay system and a TD-2020 luminometer (Promega).

2.3. Cell cycle analysis and detection of apoptosis

Cells were incubated with AG490 (100 μmol/L) and/or TRAIL (2 ng/ml) or vehicle alone (0.1% DMSO) for 24 h, fixed with 70% ethanol treated with RNase (100 μg/ml, Sigma Chemical Co., St. Louis, MO), and stained with propidium iodide (100 μg/ml, Sigma) for 30 min on ice. DNA content in the cells was analyzed by a flow cytometer (Epics XL; Beckman Coulter, Miami, FL). Apoptosis was also analyzed by ApoStrand™ ELISA apoptosis detection kit (Biomol International, PA) which detects the denatured DNA in apoptotic cells with a monoclonal antibody to single-stranded DNA.

2.4. Western blotting

Cells were lysed by addition of lysis buffer (50 mM Tris [pH 8.0], 150 mM NaCl, 0.1% SDS, 100 μg/ml PMSF, 1% NP40, 0.5% sodium deoxycholate and 1 mM sodium *o*-vanadate). Twenty micrograms of each lysate was electrophoresed on SDS–polyacrylamide gels and electrotransferred to nitrocellulose membranes, and incubated for 1 h in the presence of each of the following antibodies; mouse monoclonal anti-human phospho-(Y-705)-STAT3 (Cell Signaling, Beverly, MA), rabbit polyclonal anti-human STAT3, Bcl-xL, XIAP, survivin, cyclinD1 and Waf1/p21 (Cell Signaling), rabbit polyclonal anti-human Bax, CIAP-1 and CIAP-2 (Santa Cruz Biotechnology, Santa Cruz, CA), rabbit polyclonal anti-human FLIP (PharMingen, San Diego, CA), mouse monoclonal anti-human SOCS-1 and SOCS-3 (MBL, Nagoya, Japan), rabbit polyclonal anti-human DR4 and DR5 (Imgenex, San Diego, CA) and mouse monoclonal anti-human β-actin (Sigma) as an internal control. The membranes were washed and incubated with horseradish peroxidase-conjugated anti-rabbit IgG or anti-mouse IgG for 1 h. Immunoreactive bands were visualized by the ECL chemiluminescence system (Amersham Life Science, Buckinghamshire, UK).

2.4.1. RT-PCR

RT-PCR was performed using OneStep RT-PCR Kit (Qiagen, Valencia, CA) and Human TRAIL-R1/DR4 or TRAIL-R2/DR5 primer pairs (R&D Systems) to yield a 567-bp or 432 and 345-bp products, respectively. The amplification was performed for 30 cycles in a programmable DNA thermal cycler.

2.5. In vivo study

Five-week-old male BALB/c nu/nu athymic mice were purchased from Charles River Japan (Yokohama, Japan). Animal experiments were performed in accordance with institutional guidelines, and the study was approved by the Ethics Committee of Nagasaki University.

Huh-7 cells (3×10^6) were implanted subcutaneously into the right thigh of mice, when the tumor diameter reached 5 mm. AG490 (0.5 mg/mouse) and/or TRAIL (40 ng/mouse) was injected into the peritoneal space once a day for 13 days. As a control, 0.1 ml of vehicle (50% DMSO) was injected. Each group consisted of five mice. Tumor growth was monitored daily by measuring two perpendicular tumor diameters with a caliper, and tumor volume was calculated using a formula; (width^2 × length)/2. At the end of the study, tumors were resected from mice, weighted, and subjected to histopathological examination together with liver tissues.

2.6. Statistical analysis

Variable data were expressed as means ± SD. Differences between groups were examined for statistical significance using Student's *t* test.

3. Results

3.1. AG490 inhibits constitutive activation of STAT3 in human hepatoma cells

Constitutive phosphorylation of STAT3 at tyrosine 705 was clearly detected in all hepatoma cells, however, STAT3 was only faintly phosphorylated in normal hepatocytes (Fig. 1A). Since JAK2 is one of the major upstream activators of STAT3, we examined the effect of AG490, a JAK2 specific inhibitor, on the STAT3 phosphorylation. AG490 inhibited the phosphorylation of STAT3 in all hepatoma cells, but not in normal hepatocytes. Since SOCS-1 and SOCS-3, negative regulators of the JAK2-STAT3 signaling pathway, are silenced in several hepatoma cells [19,20], we analyzed the expression of SOCS-1 and SOCS-3 by Western blotting. SOCS-1 was detected in Huh-7 and HepG2 but not in Huh-1 or Hep3B, however, SOCS-3 was hardly detected in all hepatoma cells. In contrast, both SOCS-1 and SOCS-3 were detected in normal hepatocytes (Fig. 1B). Next, to determine the extent of constitutive activity of STAT3 in hepatoma cells, the luciferase reporter assay was carried out using a pSTAT3-TA-Luc with or without IL-6 stimulation. The luciferase activity of pSTAT3-TA-Luc without IL-6 stimulation was nearly fourfold higher than that of pTA-Luc which lacks STAT3 binding sequences, and was almost half of that of pSTAT3-TA-Luc with IL-6 stimulation in Huh-1 and Huh-7 (Fig. 1C). Whereas, AG490 dose-dependently repressed the luciferase activity of pSTAT3-TA-Luc in both cells (Fig. 1D). These results indicate that STAT3 is constitutively activated in human hepatoma cells, which is abrogated by AG490.

3.2. AG490 suppresses the growth of human hepatoma cells

We examined the effect of AG490 on the growth of hepatoma cells. AG490 dose-dependently suppressed the growth of all hepatoma cells (Fig. 2A). Next, DNA content in hepatoma cells was analyzed by a flow cytometer (Fig. 2B). In Huh-1, Huh-7 and HepG2, the percentage of both S phase and G2/M phase decreased 24 h after AG490 treatment, and the percentage of G0/G1 phase increased. Whereas, the subG1 population corresponding to the apoptotic cells increased slightly, although more than 48 h incubation with AG490 increased subG1 population more in these cells (data not shown). In contrast, the subG1 population clearly increased 24 h after AG490 treatment in Hep3B (Fig. 2B). These results indicate that the inhibition of constitutive activation of STAT3 induced cell cycle arrest at G0/G1 phase in Huh-1, Huh-7 and HepG2, and induced apoptosis in Hep3B.

To clarify whether the inhibition of STAT3 activity by means of other than AG490 can also repress the growth of hepatoma cells, a cell permeable STAT3 inhibitor peptide was used in the experiments. This phosphopeptide specifically complexes with STAT3 monomers through binding to STAT3-SH2 domain and disrupts the dimerization of STAT3 [13]. Addition of STAT3 inhibitor peptide dose-dependently repressed the luciferase activity of pSTAT3-TA-Luc in Huh-7 and their growth as well as AG490 (Fig. 3).

3.3. AG490 represses the expression of cyclin D1 and anti-apoptotic proteins in human hepatoma cells

Cyclin D1 is a key molecule stimulating G1 to S phase transition and its expression is regulated by STAT3 [2,3]. Western blotting showed that the expression of cyclin D1 was repressed in all hepatoma cells by AG490 (Fig. 4). Whereas, the expression of Waf1/p21 that inhibits G1 to S phase transition was upregulated by AG490 in Huh-7 and Hep3B. In addition, we examined the expression of several anti-apoptotic proteins. Of these, the expression of Bcl-xL and survivin, which are known as STAT3-regulated genes [2,3,5,11] and related with hepatoma development [32,33], was suppressed by AG490 in Huh-1, HepG2 and Hep3B. However, the expression of XIAP was suppressed by AG490 only in Huh-7. The expression of FLIP and CIAP-1, -2 was unchanged by AG490 in all hepatoma cells. In contrast, the expression of Bax, which has an apoptotic-promoting function, was upregulated by AG490 in Hep3B in which AG490 induced apoptosis.

3.4. AG490 sensitizes human hepatoma cells to TRAIL-induced apoptosis

We evaluated whether abrogation of STAT3 signaling by AG490 sensitized human hepatoma cells to TRAIL-induced apoptosis. 2 ng/ml of TRAIL alone slightly induced apoptosis in Huh-1, and did not induce apoptosis in Huh-7 and HepG2 (Fig. 5A). In addition, AG490 alone slightly induced apoptosis in these cells (Fig. 2B). However, the combination of AG490 and

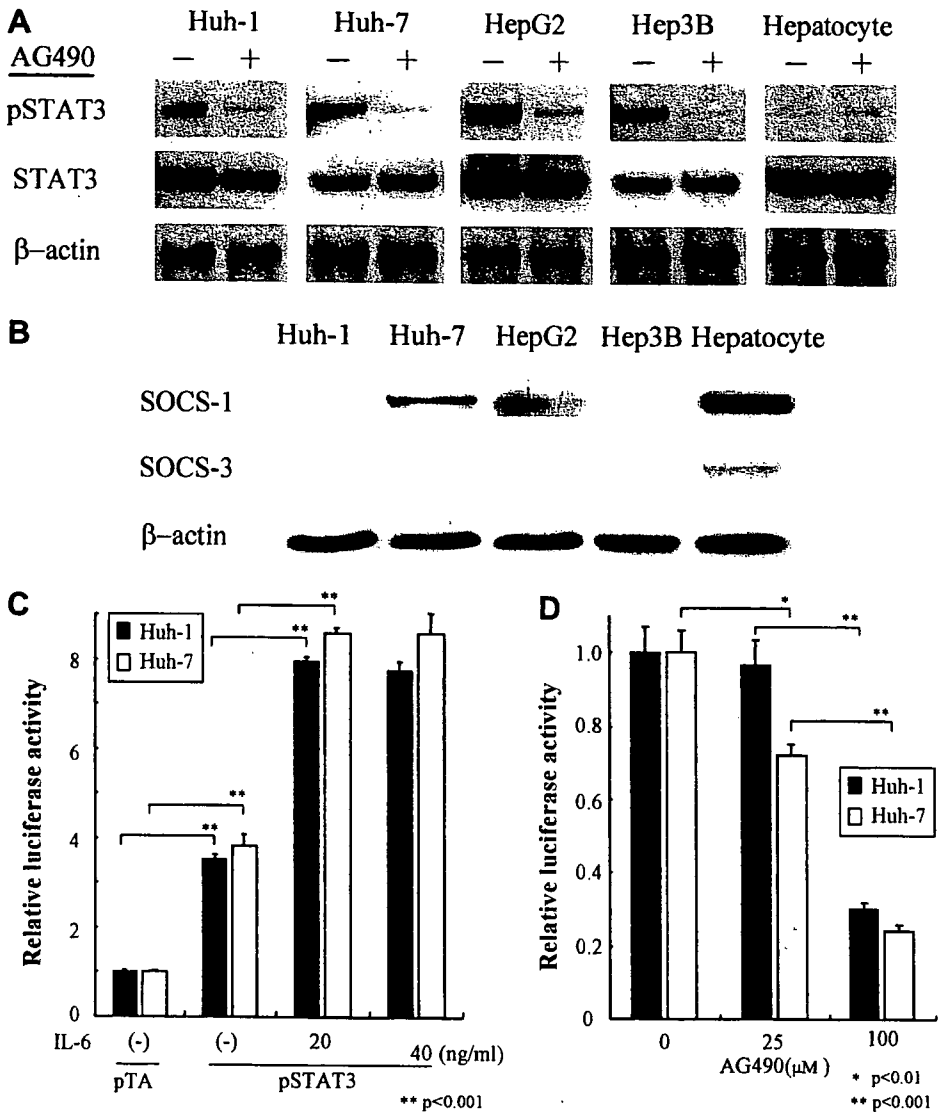

Fig. 1. Effect of AG490 on STAT3 activity in human hepatoma cells (A) Huh-1, Huh-7, HepG2, Hep3B cells and normal human hepatocytes (Hc cells) were incubated with AG490 (+) (100 μM) for 3 h or vehicle (0.1% DMSO) alone as a control (−), after which STAT3 phosphorylation at tyrosine 705 was analyzed by Western blotting. Upper, middle and lower lanes correspond to phosphorylated STAT3, total STAT3 and β-actin, respectively. Results shown are from one representative experiment from a total of four performed. (B) The expression of SOCS-1, SOCS-3 and β-actin in hepatoma cells and normal human hepatocytes (Hc cells) was analyzed by Western blotting. Results shown are from one representative experiment from a total of three performed. (C) pSTAT3-TA-Luc was cotransfected with pRL-CMV-Luc into Huh-1 (closed bar) and Huh-7 (open bar) cells. Six hours later, the cells were incubated with or without IL-6 (20 and 40 ng/ml) for 24 h. Luciferase activity in the cells was analyzed by dual-luciferase assay. Data represent ratios of firefly-Luc activity derived from pSTAT3-TA-Luc over *Renilla*-Luc activity derived from pRL-CMV-Luc relative to the control (pTA-Luc and pRL-CMV-Luc cotransfection without IL-6), and are expressed as mean ± SD of three separate experiments. (D) pSTAT3-TA-luc was cotransfected with pRL-CMV-luc into Huh-1 (closed bar) and Huh-7 (open bar) cells. Six hours later, the cells were incubated with AG490 (25 and 100 μM) for 24 h or vehicle (0.1% DMSO) alone as a control. Luciferase activity in the cells was analyzed by dual-luciferase assay. Data represent ratios of firefly-luc activity derived from pSTAT3-TA-luc over *Renilla*-luc activity derived from pRL-CMV-luc relative to the control, and are expressed as means ± SD of three separate experiments.

TRAIL apparently induced apoptosis in these cells (Fig. 5A).

Next, we determined the effect of AG490 on the expression of TRAIL death receptors, DR4 and DR5. Western blotting showed that DR5 expression was upregulated by AG490 in Huh-1 and Huh-7 but not HepG2, and that DR4 expression was upregulated in HepG2 but unchanged in other cells (Fig. 5B). RT-PCR analysis also showed the AG490-mediated upregulation of DR5 or DR4 mRNA in Huh-7 or HepG2, respectively (Fig. 5C). To know the role of AG490-mediated upregulation of DR5 or DR4, we examined the effects of DR5 and DR4-specific blocking chimera antibodies (DR5-chimera and DR4-chimera) on AG490/TRAIL-induced apoptosis in Huh-7 and HepG2 (Fig. 5D), where DR5-chimera more repressed the AG490/TRAIL-induced apoptosis in Huh-7 than DR4-chimera, in contrast, DR4-chimera more repressed

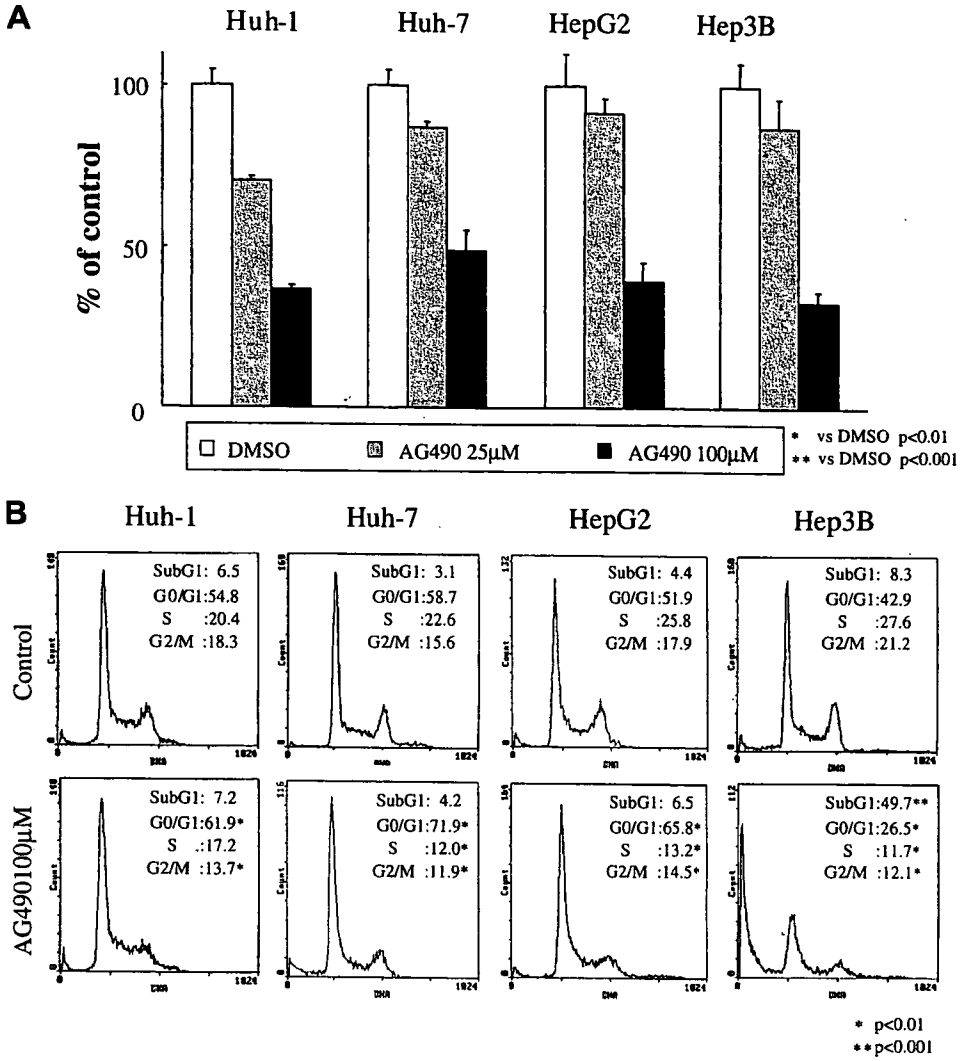

Fig. 2. Effect of AG490 on the cell growth, cell cycle and apoptosis of human hepatoma cells. (A) Huh-1, Huh-7, HepG2 and Hep3B cells were seeded into 24-well plates at a density of 2×10^4 cells per well and incubated with AG490 (25 and 100 μM) for 48 h or vehicle (0.1% DMSO) alone as a control, after which cell number was counted. Results are expressed as a percentage of the control. Data represent means ± SD values of four separate experiments. (B) Huh-1, Huh-7, HepG2 and Hep3B cells were incubated with AG490 (100 μM) for 24 h or vehicle (0.1% DMSO) alone as a control. Cells were then stained with propidium iodide and subjected to DNA content analysis by flow cytometry. Results shown are from one representative experiment from a total of four performed. The mean percentages of cells in G0/G1, S, G2/M and SubG1 from four separate experiments are indicated; $^*p < 0.01$ versus control, $^{**}p < 0.001$ versus control.

those apoptosis in HepG2 than DR5-chimera. These results suggest that AG490-mediated upregulation of DR5 in Huh-7 and DR4 in HepG2, respectively, may contribute to increased susceptibility of these cells to TRAIL.

3.5. Combination of AG490 and TRAIL inhibits the growth of pre-established Huh-7 tumor in an athymic mouse model

Huh-7 cells were subcutaneously inoculated into athymic mice. After the tumor diameter reached more than 5 mm, AG490 (0.5 mg/mouse) and/or TRAIL (40 ng/mouse) was injected into the peritoneal space for 13 days, and tumor growth was monitored (Fig. 6A). AG490-injected mice developed smaller tumor than control ($p < 0.05$) and TRAIL-injected mice ($p < 0.05$). Whereas, injection of both AG490 and TRAIL markedly repressed the growth of tumor compared to control ($p < 0.01$), TRAIL alone ($p < 0.01$) and AG490 alone ($p < 0.01$). The tumor weight at the end of the experiments in the mice treated with both AG490 and TRAIL was also significantly lighter than that in the control mice (406 ± 37 mg versus 2088 ± 285 mg, $P < 0.01$). Histopathological examination with hematoxylin-eosin (HE) staining showed that tumor cell death with condensed nuclei which could be corresponding to apoptotic cells was observed in the tumor tissue from mice treated with both AG490 and TRAIL (Figs. 6B-e and -f). The percentage of cell death

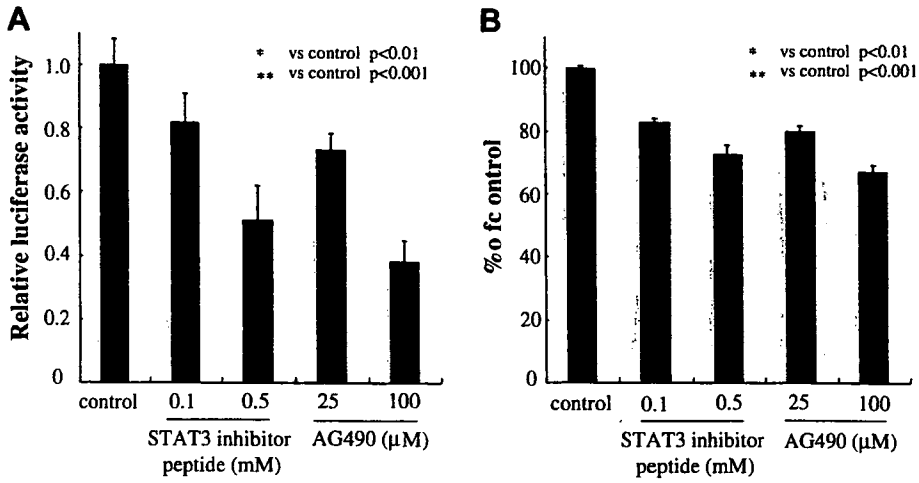

Fig. 3. Effects of STAT3 inhibitor peptide on the STAT3 activity in Huh-7 cells and their growth. (A) pSTAT3-TA-Luc was cotransfected with pRL-CMV-Luc into Huh-7 cells. Six hours later, the cells were cultured alone (control), or with STAT3 inhibitor peptide (0.1 and 0.5 mM) or AG490 (25 and 100 μM) for 24 h. Luciferase activity was determined as described in Fig. 1 legend. Data are expressed as means ± SD values of four separate experiments. (B) Huh-7 cells were cultured alone (control), or with STAT3 inhibitor peptide (0.1 and 0.5 mM) or AG490 (25 and 100 μM) for 24 h, and cell viability was determined by the colorimetric method using a Cell Counting kit (Wako Life Science, Osaka, Japan). Data represent the percentage of control, and are expressed as means ± SD values of four separate experiments.

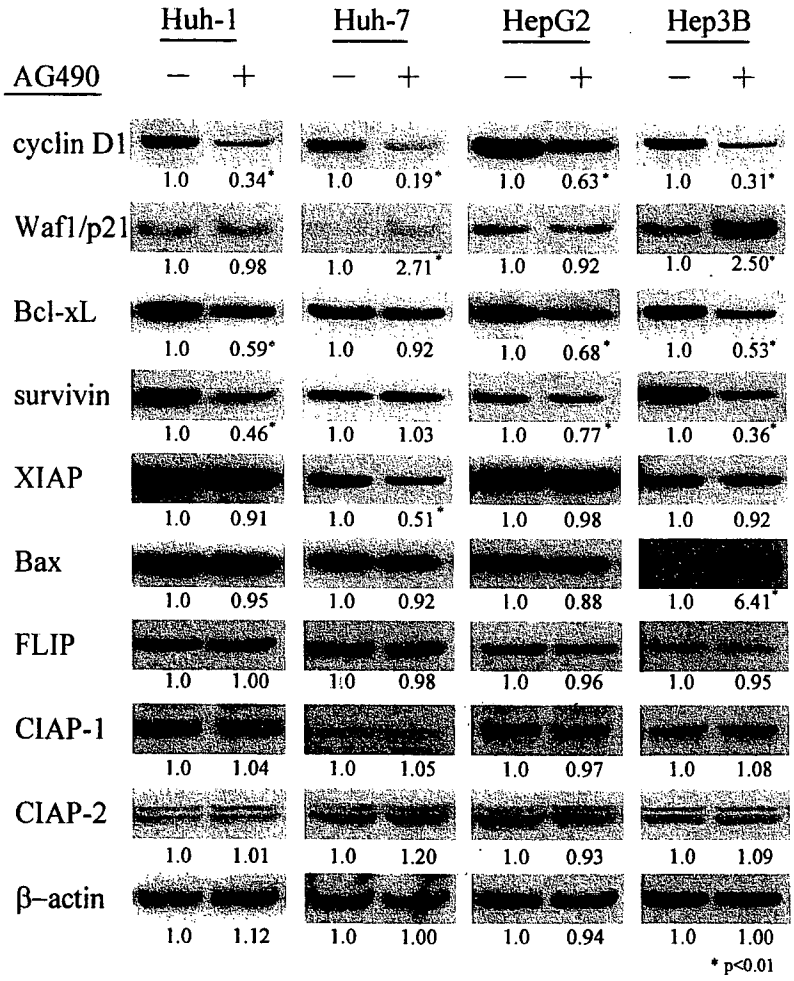

Fig. 4. Effect of AG490 on the expression of cyclin D1, Waf1/p21 and several apoptosis-related proteins in human hepatoma cells. Huh-1, Huh-7, HepG2 and Hep3B cells were incubated with AG490 (+) (100 μM) for 24 h or vehicle (0.1% DMSO) alone as a control (−), and the expression of cyclin D1, Waf1/p21, Bcl-xL, survivin, XIAP, Bax, FLIP, CIAP-1, CIAP-2 and β-actin in the cells was analyzed by Western blotting using the appropriate antibodies. Results shown are from one representative experiment from a total of four performed. The density of each band in the four separate experiments was quantified with NIH image analysis software, and the mean ratio of density relative to control (−) is indicated; *$p < 0.01$ versus control.

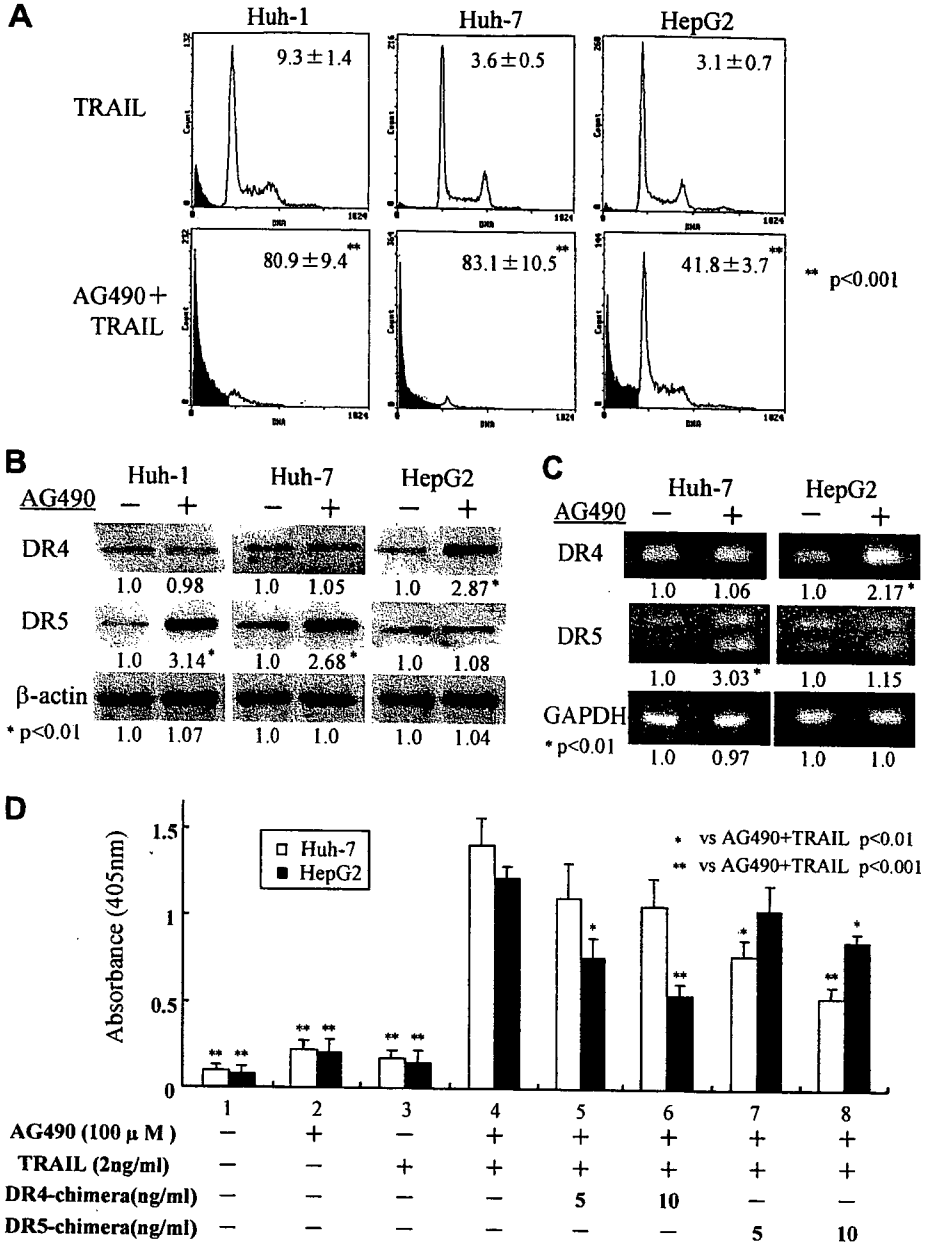

Fig. 5. Effect of AG490 on TRAIL-mediated apoptosis and the expression of DR4 and DR5 in human hepatoma cells. (A) Huh-1, Huh-7 and HepG2 cells were incubated in the presence of TRAIL (2 ng/ml) with or without AG490 (100 μM) for 24 h, and DNA contents were analyzed by flow cytometry. Histograms with black areas represent SubG1 population in the cells. Results shown are from one representative experiment from a total of four performed. Means ± SD percentages of cells in SubG1 from four separate experiments are indicated; $^{**}p < 0.001$ versus control. (B) Huh-1, Huh-7 and HepG2 cells were incubated with AG490(+) (100 μM) for 24 h or vehicle (0.1% DMSO) alone as a control (−) and the expression of DR4, DR5 and β-actin in the cells was analyzed by Western blotting. Results shown are from one representative experiment from a total of five performed. The density of each band in the five separate experiments was quantified with NIH image analysis software, and the mean ratio of density relative to control (−) is indicated; $^{*}p < 0.01$ versus control (−). (C) Huh-7 and HepG2 cells were incubated with AG490(+) (100 μM) for 24 h or vehicle (0.1% DMSO) alone as a control (−) and the m-RNA expression of DR4, DR5 and GAPDH in the cells was analyzed by RT-PCR. The PCR products were electrophoresed on a 1.2% agarose gel and visualized by ethidium bromide staining. Results shown are from one representative experiment from a total of four performed. The density of each band in the four separate experiments was quantified with NIH image analysis software, and the mean ratio of density relative to control (−) is indicated; $^{*}p < 0.01$ versus control (−). (D) Huh-7 (open bar) and HepG2 (closed bar) cells were cultured alone (control; lane 1), or with AG490 (100 μM) (lane 2), TRAIL (2 ng/ml) (lane 3), AG490 + TRAIL (lane 4), AG490 + TRAIL + DR4-chimera; 5 ng/ml (lane 5) or 10 ng/ml (lane 6), AG490 + TRAIL + DR5-chimera; 5 ng/ml (lane 7) or 10 ng/ml (lane 8) for 18 h in 96-well microplates, and apoptotic cells were analyzed by ApoStrand™ ELISA apoptosis detection kit including anti-ssDNA monoclonal antibody and peroxidase-conjugated anti-mouse antibody. Data represent absorbance (405 nm), and are expressed as means ± SD values of four separate experiments.

area measured from HE staining was significantly higher in the tumor tissue from mice treated with AG490 and TRAIL than that from control mice; 58.5 ± 7.4% vs 8.8 ± 3.1%, $p < 0.01$. In contrast, the damage of normal hepatocytes was hardly observed in mice treated with AG490 and TRAIL (Figs. 6B-b and -c) although HE

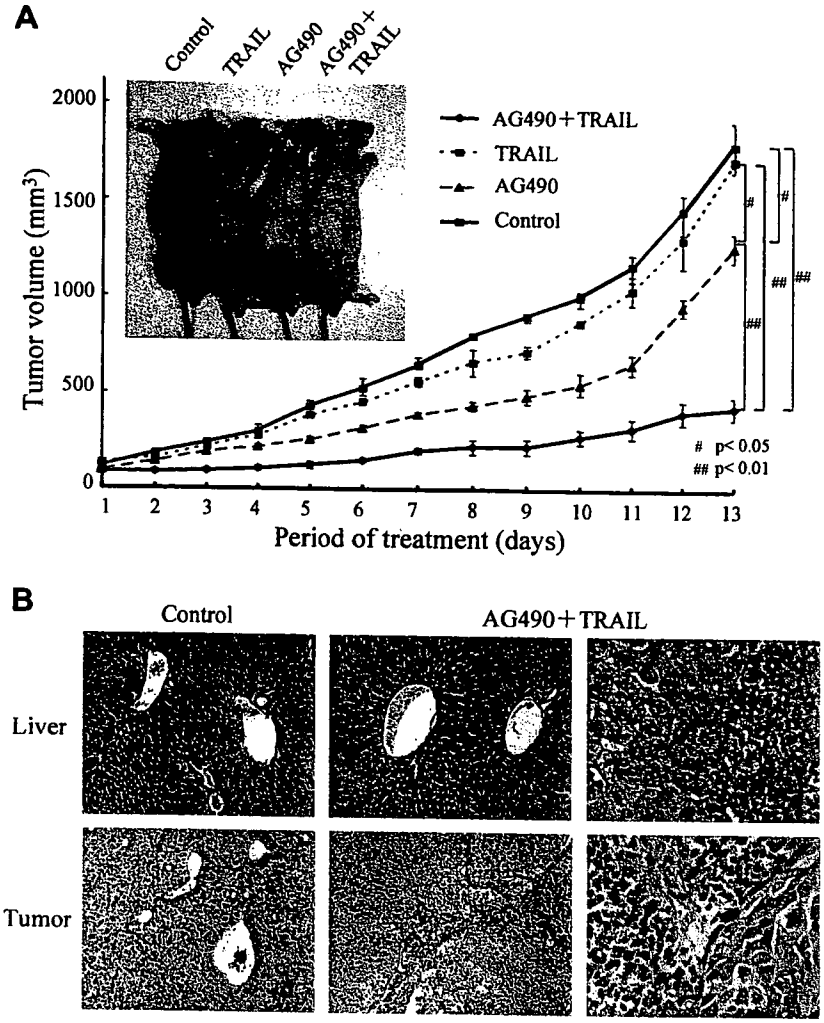

Fig. 6. Anti-tumor effect of combination of AG490 and TRAIL in xenograft models. (A) Huh-7 cells were implanted into athymic mice subcutaneously, and, when tumor diameter reached 5 mm, mice were treated with intraperitoneal injection of vehicle (0.1 ml of 50% DMSO) alone as a control, AG490 (0.5 mg/mouse), TRAIL (40 ng/mouse), and both AG490 (0.5 mg/mouse) and TRAIL (40 ng/mouse) for 13 days, respectively, then tumor growth was monitored as described in Section 2. Data represent means ± SD; *$p < 0.01$ versus control, AG490 alone or TRAIL alone, respectively. Representative photograph of mice after each treatment is also shown. (B) Hematoxylin–eosin (HE) staining of tumors and liver tissues resected from control mouse or mouse treated with both AG490 and TRAIL is shown. a, liver of control mouse; b, liver of mouse treated with both AG490 and TRAIL; c, high magnification of b; d, tumor of control mouse; e, tumor of mouse treated with both AG490 and TRAIL; f, high magnification of e. The percentage of cell death area in each HE-stained tumor specimen was measured with Scion Image (Scion Corporation, Maryland, USA).

staining is not enough to convince the safety of AG490 and TRAIL treatment.

4. Discussion

In the present study, SOCS-1 was silenced in Huh-1 and Hep3B, but not in Huh-7 and HepG2, whereas, SOCS-3 was silenced in all hepatoma cells. In contrast, both SOCS-1 and SOCS-3 were detected in normal human hepatocytes in which the level of STAT3 phosphorylation at tyrosine 705 was much lower than that in hepatoma cells. Taken together, it is possible that both SOCS-1 and SOCS-3 are required for negatively regulating the level of STAT3 phosphorylation in hepatocytes.

Recent studies have shown that src family kinases mediate constitutive STAT3 activation rather than JAK2 in several cancer cells [34–36], and that growth factor receptors such as epidermal growth factor receptor (EGFR) and c-met activate STAT3 through src family kinases [37,38], whereas AG490, a JAK2 specific inhibitor, failed to inhibit the constitutive activation of STAT3 but the src specific inhibitor did. In our study, however, AG490 inhibited the phosphorylation of STAT3 and its transcriptional activity, suggesting that JAK2 is the key kinase involved in the constitutive activation of STAT3 in human hepatoma cells.

Several target genes of STAT3 have been identified including cyclin D1, Bcl-xL, Bcl-2, survivin, mcl-1, c-myc and vascular endothelial growth factor (VEGF) [2–6,12,39] that are essential for cell growth and

survival. These findings are consistent with the reports that abrogation of STAT3 signaling inhibit the growth of various cancer cells and induce apoptosis [9–15]. In the present study, AG490 not only downregulated the expression of cyclin D1 in all hepatoma cells but also upregulated the expression of Waf1/p21 in Huh-7 and Hep3B as reported previously [12], resulting in cell cycle arrest at the G0/G1 phase in Huh-1, Huh-7 and HepG2. On the other hand, AG490 induced apoptosis in Hep3B in which Bax expression was upregulated. In addition, AG490 downregualated the expression of at least one of the anti-apoptotic proteins, Bcl-xL, survivin or XIAP, in all hepatoma cells.

Recent studies have shown that abrogation of STAT3 signaling sensitized cancer cells to chemotherapeutic agents [39,40] and interleukin-12 [41], and that STAT3-inactivated keratinocytes become sensitive to UV-induced apoptosis [42], suggesting that STAT3 signaling pathway protects the cells from various apoptosis stimuli. Therefore, we evaluated whether AG490 sensitized human hepatoma cells to TRAIL-induced apoptosis. TRAIL has been known as a tumor-specific death ligand, however, several cancer cells including hepatoma cells are resistant to TRAIL-induced apoptosis [27]. We have previously reported that interferon (IFN)-α sensitizes human hepatoma cells to TRAIL-induced apoptosis through downregulation of survivin and through upregulation of DR5, a death receptor of TRAIL [43]. In the present study, combination of AG490 and TRAIL apparently induced apoptosis in human hepatoma cells and repressed the growth of Huh-7 tumor in the xenograft model, which could be explained by AG490-mediated downregulation of anti-apoptotic proteins such as Bcl-xL, survivin or XIAP and upregulation of DR4 or DR5 in these cells. Of these, upregulation of DR4 or DR5 by AG490 appears to be essential for increased susceptibility of hepatoma cells to TRAIL because blocking of DR4 or DR5-mediated death signaling by its specific chimera antibody inhibited the synergistic effects of AG490 and TRAIL in inducing apoptosis. However, AG490 did not equally affect the expression of these proteins in hepatoma cells. Furthermore, we only examined the effect of AG490 on the expression of a limited number of cell cycle-related or apoptosis-related proteins. In this regard, Alvarez et al. have recently investigated STAT3 target genes cyclopaedically using microarray analysis and found the rapid induction (within 4.5 h) of several transcription factors including junB, egr1, KLF4, bcl-6 and NFIL3 by STAT3, and proposed that large number of genes are secondarily stimulated by these transcription factors [44]. Surprisingly, they have also revealed that cyclin D1, Bcl-xL and c-myc were not activated by STAT3 at the 4.5 h time point, and speculated that the protein products of other STAT3 target genes are required to collaborate with STAT3 to activate expression of cyclin D1, Bcl-xL and c-myc [44]. Their speculation may also explain the varying effects of AG490 on the expression of apoptosis-related proteins in our study because this expression could be indirectly influenced by AG490 through widespread changes in cellular conditions, which are probably not equivalent in each hepatoma cell.

In conclusion, we have demonstrated in the present study that abrogation of constitutive activation of STAT3 by AG490, JAK2 specific inhibitor, repressed the growth of human hepatoma cells *in vitro*, and greatly enhanced the anti-tumor activity of TRAIL against these cells both *in vitro* and *in vivo* without any adverse effect on normal hepatocytes. These results suggest that the combination of AG490 and TRAIL may have therapeutic potential in the treatment of human HCC.

References

[1] Aaronson DS, Horvath CM. A road map for those who don't know JAK-STAT. Science 2002;296:1653–1655.
[2] Bowman T, Garcia R, Turkson J, Jove R. STATs in oncogenesis. Oncogene 2000;19:2474–2488.
[3] Buettner R, Mora LB, Jove R. Activated STAT signaling in human tumors provides novel molecular targets for therapeutic intervention. Clin Cancer Res 2002;8:945–954.
[4] Wei D, Le X, Zheng L, Wang L, Frey JA, Gao AC, et al. Stat3 activation regulates the expression of vascular endothelial growth factor and human pancreatic cancer angiogenesis and metastasis. Oncogene 2003;22:319–329.
[5] Kanda N, Seno H, Konda Y, Marusawa H, Kanai M, Nakajima T, et al. STAT3 is constitutively activated and supports cell survival in association with survivin expression in gastric cancer cells. Oncogene 2004;23:4921–4929.
[6] Clevenger CV. Roles and regulation of stat family transcription factors in human breast cancer. Am J Pathol 2004;165:1449–1460.
[7] Kusaba T, Nakayama T, Yamazumi K, Yakata Y, Yoshizaki A, Nagayasu T, et al. Expression of p-STAT3 in human colorectal adenocarcinoma and adenoma; correlation with clinicopathological factors. J Clin Pathol 2005;58:833–838.
[8] Hirano T, Ishihara K, Hibi M. Roles of STAT3 in mediating the cell growth, differentiation and survival signals relayed through the IL-6 family of cytokine receptors. Oncogene 2000;19:2548–2556.
[9] Burke WM, Jin X, Lin HJ, Huang M, Liu R, Reynolds RK, et al. Inhibition of constitutively active Stat3 suppresses growth of human ovarian and breast cancer cells. Oncogene 2001;20:7925–7934.
[10] Rahaman SO, Harbor PC, Chernova O, Barnett GH, Vogelbaum MA, Haque SJ. Inhibition of constitutively active Stat3 suppresses proliferation and induces apoptosis in glioblastoma multiforme cells. Oncogene 2002;21:8404–8413.
[11] Aoki Y, Feldman GM, Tosato G. Inhibition of STAT3 signaling induces apoptosis and decreases survivin expression in primary effusion lymphoma. Blood 2003;101:1535–1542.
[12] Scholz A, Heinze S, Detjen KM, Peters M, Welzel M, Hauff P, et al. Activated signal transducer and activator of transcription 3 (STAT3) supports the malignant phenotype of human pancreatic cancer. Gastroenterology 2003;125:891–905.
[13] Turkson J, Ryan D, Kim JS, Zhang Y, Chen Z, Haura E, et al. Phosphotyrosyl peptides block Stat3-mediated DNA binding

activity, gene regulation, and cell transformation. J Biol Chem 2001;276:45443–45455.
[14] Leong PL, Andrews GA, Johnson DE, Dyer KF, Xi S, Mai JC, et al. Targeted inhibition of Stat3 with a decoy oligonucleotide abrogates head and neck cancer cell growth. Proc Natl Acad Sci USA 2003;100:4138–4143.
[15] Mora LB, Buettner R, Seigne J, Diaz J, Ahmad N, Garcia R, et al. Constitutive activation of Stat3 in human prostate tumors and cell lines: direct inhibition of Stat3 signaling induces apoptosis of prostate cancer cells. Cancer Res 2002;62:6659–6666.
[16] Chan KS, Sano S, Kiguchi K, Anders J, Komazawa N, Takeda J, et al. Disruption of Stat3 reveals a critical role in both the initiation and the promotion stages of epithelial carcinogenesis. J Clin Invest 2004;114:720–728.
[17] Tiollais P, Pourcel C, Dejean A. The hepatitis B virus. Nature 1985;317:489–495.
[18] Kiyosawa K, Sodeyama T, Tanaka E, Gibo Y, Yoshizawa K, Nakano Y, et al. Interrelationship of blood transfusion, non-A, non-B hepatitis and hepatocellular carcinoma: analysis by detection of antibody to hepatitis C virus. Hepatology 1990;12:671–675.
[19] Yoshikawa H, Matsubara K, Qian GS, Jackson P, Groopman JD, Manning JE, et al. SOCS-1, a negative regulator of the JAK/STAT pathway, is silenced by methylation in human hepatocellular carcinoma and shows growth-suppression activity. Nat Genet 2001;28:29–35.
[20] Niwa Y, Kanda H, Shikauchi Y, Saiura A, Matsubara K, Kitagawa T, et al. Methylation silencing of SOCS-3 promotes cell growth and migration by enhancing JAK/STAT and FAK signalings in human hepatocellular carcinoma. Oncogene 2005;24:6406–6417.
[21] Feng DY, Zheng H, Tan Y, Cheng RX. Effect of phosphorylation of MAPK and Stat3 and expression of c-fos and c-jun proteins on hepatocarcinogenesis and their clinical significance. World J Gastroenterol 2001;7:33–36.
[22] Liu P, Kimmoun E, Legrand A, Sauvanet A, Degott C, Lardeux B, et al. Activation of NF-kappa B, AP-1 and STAT transcription factors is a frequent and early event in human hepatocellular carcinomas. J Hepatol 2002;37:63–71.
[23] Waris G, Turkson J, Hassanein T, Siddiqui A. Hepatitis C virus (HCV) constitutively activates STAT-3 via oxidative stress: role of STAT-3 in HCV replication. J Virol 2005;79:1569–1580.
[24] Yoshida T, Hanada T, Tokuhisa T, Kosai K, Sata M, Kohara M, et al. Activation of STAT3 by the hepatitis C virus core protein leads to cellular transformation. J Exp Med 2002;196:641–653.
[25] Walczak H, Miller RE, Ariail K, Gliniak B, Griffith TS, Kubin M, et al. Tumoricidal activity of tumor necrosis factor-related apoptosis-inducing ligand in vivo. Nat Med 1999;5:157–163.
[26] Ashkenazi A, Pai RC, Fong S, Leung S, Lawrence DA, Marsters SA, et al. Safety and antitumor activity of recombinant soluble Apo2 ligand. J Clin Invest 1999;104:155–162.
[27] Yamanaka T, Shiraki K, Sugimoto K, Ito T, Fujikawa K, Ito M, et al. Chemotherapeutic agents augment TRAIL-induced apoptosis in human hepatocellular carcinoma cell lines. Hepatology 2000;32:482–490.
[28] Lacour S, Hammann A, Wotawa A, Corcos L, Solary E, Dimanche-Boitrel MT. Anticancer agents sensitize tumor cells to tumor necrosis factor-related apoptosis-inducing ligand-mediated caspase-8 activation and apoptosis. Cancer Res 2001;61:1645–1651.
[29] Chinnaiyan AM, Prasad U, Shankar S, Hamstra DA, Shanaiah M, Chenevert TL, et al. Combined effect of tumor necrosis factor-related apoptosis-inducing ligand and ionizing radiation in breast cancer therapy. Proc Natl Acad Sci USA 2000;97:1754–1759.
[30] Nakabayashi H, Taketa K, Yamane T, Miyazaki M, Miyano K, Sato J. Phenotypical stability of a human hepatoma cell line, HuH-7, in long-term culture with chemically defined medium. Gann 1984;75:151–158.
[31] Osawa Y, Banno Y, Nagaki M, Brenner DA, Naiki T, Nozawa Y, et al. TNF-alpha-induced sphingosine 1-phosphate inhibits apoptosis through a phosphatidylinositol 3-kinase/Akt pathway in human hepatocytes. J Immunol 2001;167:173–180.
[32] Takehara T, Liu X, Fujimoto J, Friedman SL, Takahashi H. Expression and role of Bcl-xL in human hepatocellular carcinomas. Hepatology 2001;34:55–61.
[33] Notarbartolo M, Cervello M, Giannitrapani L, Meli M, Poma P, Dusonchet L, et al. Expression of IAPs and alternative splice variants in hepatocellular carcinoma tissues and cells. Ann N Y Acad Sci 2004;1028:289–293.
[34] Niu G, Bowman T, Huang M, Shivers S, Reintgen D, Daud A, et al. Roles of activated Src and Stat3 signaling in melanoma tumor cell growth. Oncogene 2002;21:7001–7010.
[35] Xi S, Zhang Q, Dyer KF, Lerner EC, Smithgall TE, Gooding WE, et al. Src kinases mediate STAT growth pathways in squamous cell carcinoma of the head and neck. J Biol Chem 2003;278:31574–31583.
[36] Laird AD, Li G, Moss KG, Blake RA, Broome MA, Cherrington JM, et al. Src family kinase activity is required for signal transducer and activator of transcription 3 and focal adhesion kinase phosphorylation and vascular endothelial growth factor signaling in vivo and for anchorage-dependent and -independent growth of human tumor cells. Mol Cancer Ther 2003;2:461–469.
[37] Song L, Turkson J, Karras JG, Jove R, Haura EB. Activation of Stat3 by receptor tyrosine kinases and cytokines regulates survival in human non-small cell carcinoma cells. Oncogene 2003;22:4150–4165.
[38] Silva CM. Role of STATs as downstream signal transducers in Src family kinase-mediated tumorigenesis. Oncogene 2004;23:8017–8023.
[39] Real PJ, Sierra A, De Juan A, Segovia JC, Lopez-Vega JM, Fernandez-Luna JL. Resistance to chemotherapy via Stat3-dependent overexpression of Bcl-2 in metastatic breast cancer cells. Oncogene 2002;21:7611–7618.
[40] Alas S, Bonavida B. Inhibition of constitutive STAT3 activity sensitizes resistant non-Hodgkin's lymphoma and multiple myeloma to chemotherapeutic drug-mediated apoptosis. Clin Cancer Res 2003;9:316–326.
[41] Burdelya L, Catlett-Falcone R, Levitzki A, Cheng F, Mora LB, Sotomayor E, et al. Combination therapy with AG-490 and interleukin 12 achieves greater antitumor effects than either agent alone. Mol Cancer Ther 2002;1:893–899.
[42] Sano S, Chan KS, Kira M, Kataoka K, Takagi S, Tarutani M, et al. Signal transducer and activator of transcription 3 is a key regulator of keratinocyte survival and proliferation following UV irradiation. Cancer Res 2005;65:5720–5729.
[43] Shigeno M, Nakao K, Ichikawa T, Suzuki K, Kawakami A, Abiru S, et al. Interferon-alpha sensitizes human hepatoma cells to TRAIL-induced apoptosis through DR5 upregulation and NF-kappa B inactivation. Oncogene 2003;22:1653–1662.
[44] Alvarez JV, Febbo PG, Ramaswamy S, Loda M, Richardson A, Frank DA. Identification of a genetic signature of activated signal transducer and activator of transcription 3 in human tumors. Cancer Res 2005;65:5054–5062.

Hep Intl (2007) 1:287–294
DOI 10.1007/s12072-007-9007-4

ORIGINAL PAPER

Role of growth hormone, insulin-like growth factor 1 and insulin-like growth factor-binding protein 3 in development of non-alcoholic fatty liver disease

Tatsuki Ichikawa · Kazuhiko Nakao · Keisuke Hamasaki · Ryuji Furukawa · Shotarou Tsuruta · Yasuo Ueda · Naota Taura · Hidetaka Shibata · Masumi Fujimoto · Kan Toriyama · Katsumi Eguchi

Received: 14 April 2007 / Published online: 1 June 2007

Abstract
Background and aims Pituitary dysfunction including growth hormone (GH) deficiency may be associated with non-alcoholic fatty liver disease (NAFLD). Since the relationships among GH, IGF-1, IGFBP-3, and development of NAFLD without hypopituitarism are unclear, we examined the role of these hormones in the development of NAFLD based on clinical, laboratory and liver histology data.
Patients and methods A total of 55 consecutive patients (20 males and 35 females) with NAFLD.
Results Aspartate amino transferase (AST), AST/ALT, platelet count and IGF-1, levels were significantly associated with differences in fibrosis, since these variables differed between stage 0–1 and stage 2–3 NAFLD. In multivariate analysis, platelet count ($P = 0.0223$, relative risk (RR), 5.899; 95% confidence interval (CI), 1.288–27.017), and IGF-1 ($P = 0.0363$, RR, 4.568; 95% CI, 1.101–18.945) showed significant associations with stage 2–3 NAFLD. Additionally, hyaluronic acid levels had a negative relationship with IGF-1 and the IGF-1/IGFBP-3 ratio. There was no relationship of fibrosis with GH level, but decreased GH ($P = 0.0414$, RR, 0.199; 95% CI, 0.042–0.989) was significantly associated with steatosis of stage 2–3. Low GH/IGF-1 and GH/IGFBP-3 ratios were found in advanced steatosis.
Conclusion GH, IGF-1 and IGFBP-3 are associated with hepatic fibrosis and steatosis in NAFLD. Low levels of IGF-1 might be associated with fibrosis while low level of GH with hepatic steatosis.

Keywords Non-alcoholic fatty liver disease · Growth hormone · Insulin-like growth factor 1 · Insulin-like growth factor-binding protein 3 · Stage

Abbreviations

ALP	Alkaline phosphatase
ALT	Alanine aminotransferase
AST	Aspartate aminotransferase
γ-GTP	γ-Glutamyltranspeptidase
BMI	Body mass index
CT	Computed tomography
FMV	Flow-mediated vasodilatation
GH	Growth hormone
IGF-1	Insulin-like growth factor 1
IGFBP-3	Insulin-like growth factor-binding protein 3
IMT	Intima-media thickness
NAFLD	Non-alcoholic fatty liver disease
NASH	Non-alcoholic steatohepatitis
STAT	Signal transducers and activators of transcription
US	Ultrasonography

Introduction

Striking similarities exist between the metabolic syndrome and untreated GH deficiency (GHD) in adults, and

T. Ichikawa (✉) · K. Nakao · K. Hamasaki · N. Taura · H. Shibata · M. Fujimoto · K. Eguchi
The First department of Internal Medicine, Graduate school of Biomedical science, Nagasaki University, 1-7-1 Sakamoto, Nagasaki 852-8501, Japan
e-mail: ichikawa@net.nagasaki-u.ac.jp

R. Furukawa · S. Tsuruta · Y. Ueda
Department of Internal Medicine, The Japanese Red Cross Nagasaki Atomic Bomb Hospital, Nagasaki, Japan

K. Toriyama
Department of Pathology, Institute of Tropical medicine, Nagasaki University, Nagasaki, Japan

undetectable and low levels of GH may be of importance in the metabolic aberrations observed in both conditions [1]. Together with atherosclerosis, visceral obesity, hypertension, hyperlipidemia, and insulin resistance. Non-alcoholic fatty liver disease (NAFLD) is a common feature in metabolic syndrome and in hypopituitaric and hypothalamic dysfunction [2, 3]. Lonardo et al. showed that low levels of GH are independent predictors of NAFLD in male patients [4], and recent reports suggest that hypothalamic and/or pituitary disease including GHD involves a rapid progressive NAFLD [3]; the reason for rapid progression was speculated to be body weight gain, and not GHD itself. We have previously found an association of adult onset GHD with NAFLD [2], and shown that hepatic steatosis is more frequently observed in patients with GHD than in those without GHD, suggesting that adult onset GHD is a possible risk factor for NAFLD. However, the role of GH in NAFLD remains unclear, despite the growing knowledge of the activity of this hormone in induction of lipolysis and lipid oxidation [5].

IGF-1 is secreted from hepatocytes by GH stimulation. It is a catabolic hormone with a role in protein synthesis, and can also stimulate secretion of IGFBP-3 from Kupffer cells [6]. The biological activity of IGF-1 is strongly influenced by several IGF-specific binding proteins (IGFBP-1 to 6), of which IGFBP-3 carries >80% of circulating IGF-1 [7]. The presence of IGFBP-3 lowers IGF-1 bioactivity [8], and the ratio between IGF-1 and IGFBP-3 levels decreases with increasing age in adults, resulting in decreased levels of free and biologically active IGF-1 [9]. IGF-1 has been shown to have a protective effect on ischemic heart disease, cardiovascular disease mortality and atherosclerosis [7, 10, 11], whereas high levels of IGFBP-3 and a low IGF-1/IGFBP-3 ratio are correlated with atherosclerosis [9]. Cardiovascular disease is a serious problem in NAFLD patients, and ischemic heart disease is a major cause of death among these patients [12]. NAFLD is associated with advanced carotid atherosclerosis [13] and endothelial dysfunction, and the 10-year probability of occurrence of cardiovascular events [14], and especially intima-media thickness (IMT) has a strong association with the degree of hepatic fibrosis in NAFLD patients [15].

Although GH levels have been correlated with metabolic syndrome, and IGF-1 and IGFBP-3 are related to cardiovascular disease, the relationships among GH, IGF-1, IGFBP-3, and the severity of NAFLD have not been examined. Therefore, the aim of this study was to compare GH, IGF-1, and IGFBP-3 levels with the degree of fibrosis, inflammation and steatosis in NAFLD patients, and to clarify the relationship between the development of NAFLD and the levels of these hormones.

Patients and methods

Patients

The study included 55 consecutive patients (20 males and 35 females) with NAFLD who attended the First Department of Internal Medicine at the Graduate School of Biomedical Science, Nagasaki University and the Department of Internal Medicine at the Japanese Red Cross Nagasaki Atomic Bomb Hospital, with an initial visit between April 1998 and December 2005. NAFLD was diagnosed on the basis of a persistently raised ALT level (>1.5 times the upper normal limit for 6 months or more) and on US and CT images. A percutaneous liver biopsy assisted by US was performed in all cases, and scored using the criteria proposed by Brunt et al. [16]. Liver biopsy specimens were fixed in 10% formalin, embedded in paraffin, cut to a thickness of 4 μm, and subjected to hematoxylin-eosin, and Azan-Mallory staining. All liver tissue specimens were evaluated by a single pathologist who was blinded to the clinical condition of the patient. Patients with positive hepatitis B and C serology or with evidence of inherited, autoimmune, cholestatic, or drug-induced liver disease were excluded using standard clinical, laboratory, imaging, and histological criteria. In addition, the subjects included in the study had no history of current or past excessive alcohol intake, as defined by an average daily consumption of more than 20 g of alcohol. At the time of the study, none of the patients showed clinical, biochemical or histological evidence of cirrhosis. Of the 55 cases that were originally included in the study, three secondary cases of NAFLD were subsequently excluded: two of these cases were steatohepatitis after pancreatoduodenal resection, and the third was a case of adult onset hypopituitarism.

Clinical and laboratory measurements

Body mass index (BMI) was calculated as weight (kg) divided by the square of height (m). Subjects fasted overnight before blood samples were obtained. Venous plasma glucose was measured with an automated analyzer, and basal serum insulin was measured using a standard radioimmunoassay. The index of insulin resistance was calculated using the fasting value of plasma glucose, (we excluded the patients with greater than 130 mg/dl), and the serum insulin level, according to the homeostasis model assessment (HOMA) method. Hemoglobin A1c, ALT, AST, γ-GTP, ALP, total cholesterol, triglyceride, C-reactive protein and ferritin, and hyaluronic acid were determined by standard hematometry and laboratory techniques. Measurements of GH, IGF-1. and IGFBP-3 were performed using commercially available kits. The sensitivity